DETECTION AND OPPORTUNISTIC SPECTRUM ACCESS IN SENSOR NETWORKS

by

HUNG DINH LY

Presented to the Faculty of the Graduate School of

The University of Texas at Arlington in Partial Fulfillment

of the Requirements

for the Degree of

MASTER OF SCIENCE IN ELECTRICAL ENGINEERING

THE UNIVERSITY OF TEXAS AT ARLINGTON

August 2007

To my family

ACKNOWLEDGEMENTS

I would like to express my deep gratitude to my supervising professor, Dr. Qilian Liang, for constantly motivating and encouraging me, and also for his invaluable advice during my studies at the University of Texas at Arlington (UTA). I am very grateful to the members of my thesis committee, Dr. Jonathan Bredow and Dr. Mingyu Lu, for their interest in my research and for taking time to serve on my committee.

I would like to extend my appreciation to the Vietnamese Government and Vietnam's Ministry of Education and Training (MOET) for providing financial support for my Master's studies. This financial source helps me pursue my study and research at UTA and complete this thesis.

My appreciation also goes to my friends at the VNatUTA group as well as my colleagues at the Wireless Communications and Networking Laboratory for their friendship and encouragement.

I am indebted to all the teachers who taught me during the years I spent in school. I would like to thank Dr. Nguyen Kim Lan, Dr. Bui Trung Hieu, and Dr. Nguyen Pham Anh Dung for their encouragement and inspiration.

Nothing can really express my feelings and gratitude towards my dear parents and my younger brother for their unconditional love, patience, and encouragement. It would be impossible to follow my studies without their support.

Finally, I would like to express my deepest gratitude to my lovely wife for her constant love, encouragement, and support. She has made my life more durable and fulfilled.

July 16, 2007

ABSTRACT

DETECTION AND OPPORTUNISTIC SPECTRUM ACCESS IN SENSOR NETWORKS

Publication No. _____

Hung Dinh Ly, M.S.

The University of Texas at Arlington, 2007

Supervising Professor: Dr. Qilian Liang

This thesis examines target detection problems in Radar Sensor Networks (RSN) and opportunistic spectrum access problem in Cognitive Sensor Networks (CSN). First, studies on the Space-Time Adaptive Processing (STAP) and radar waveform design are provided. Investigation into the target detection performance gain of RSN when STAP and radar waveform design are combined in RSN is then performed. Studies in this thesis show that detection performance of RSN using our proposal is superior to that of a single radar system using STAP only. To further studies on target detection, the multi-target detection problem in RSN is also examined. Signal, interference, and noise at radar sensors are modeled and analyzed. At the clusterhead of RSN, a Maximum Likelihood Multi-Target Detection algorithm is proposed to estimate the possible number of targets in a surveillance area. Achieved results show that detection performance of RSN is much better than that of a single radar system in terms of the miss-detection probability and the root mean square error.

Besides detection in RSN, this thesis studies an opportunistic spectrum access problem and proposes a spectrum access scheme in CSN. The spectrum access scheme is built using Fuzzy Logic System (FLS); and spectrum access decision is based on: (1)

spectrum utilization efficiency of the secondary user (SU); (2) its degree of mobility; and (3) its average distance to primary users (PU). The output of the FLS provides the probabilities of accessing spectrum band for SUs and the SU with the highest probability will be assigned the available spectrum. Studies also show that our scheme performs much better than random access approach.

TABLE OF CONTENTS

LIST OF FIGURES

LIST OF TABLES

CHAPTER 1

INTRODUCTION

1.1 Introduction

1.1.1 Radar Sensor Networks

Radar sensor networks (RSN) consist of collaboratively operating radar sensors which are deployed ubiquitously (possibly randomly placed) on airborne, surface, and sub-surface unmanned vehicles. Radar sensors have capabilities of doing radar sensing, signal processing, and wireless communication. Autonomous radar sensors operating in the microwave spectrum are used to detect, classify, and track visible, obscured targets at the presence of both noise and interference (clutter, jamming, and interference between sensors). RSN has advantages compared to a single radar system in improving the system sensitivity, reducing obscuration effects and vulnerability, and increasing the detection performance [42], [4].

In radar sensor networks, radar sensors are networked together in an ad-hoc fashion, i.e., they do not depend on any preexisting infrastructure. They are self-organizing entities that are deployed on demand in support of various events such as surveillance, battlefield, disaster relief, search and rescue, etc. Therefore, the network of radar sensors should operate with multiple goals managed by an intelligent platform network that can manage the dynamics of each radar to meet the common goals of the platform rather than each radar to operate as an independent system [30]. It is significant to perform signal design, signal processing, and networking cooperatively within and between platforms of radar sensors and their communication modules.

Radar sensors receive signals which are reflected from targets and embedded in interference and noise. Then, these measurements from radar sensors are wirelessly forwarded to the central processor, where measurement data are processed and combined,

to perform important applications such as detection, classification, recognition, tracking, etc. This thesis focuses on the detection problem: (1) improving the detection performance using our proposed diversity scheme in RSN, which is presented in Chapter 2; and (2) solving the multi-target detection problem in RSN, which is discussed in Chapter 3.

1.1.2 Cognitive Sensor Networks

Cognitive sensor networks (CSN) are networks of sensors equipped with cognitive radios. It has been seen that cognitive radios enables sensor networks or XG networks to use spectrum efficiently by allowing secondary (cognitive) users to opportunistically sense and utilize used spectrum. Cognitive radios have two intrinsic characteristics [41]:

- Cognitive capability: Cognitive capability implies the ability of CRs to sense information from their surroundings to find spectrum portions that are unused by primary users at a specific time or location. The most suitable CR will be selected for communications without causing harmful interference to other users.
- Reconfigurability: Reconfigurability enables CRs to be dynamically reprogrammed according to the real environment. This means that CRs can change the operating frequencies, modulation schemes, transmission powers, communication protocols, etc. on the fly without any modification of hardware components.

Cognitive radios, in order to use spectrum opportunistically, experience four main procedures, i.e.,

1. Spectrum sensing: CRs monitor spectrum bands and detect unused bands which are location-dependent and time-varying.
2. Spectrum access: Assume that multiple CRs trying to use the spectrum coexist in an area. This procedure is used to prevent multiple users from colliding in overlapping spectrum portions.
3. Communications: Once CRs get the assigned spectrum bands, they will inform their receivers about the chosen bands. After receiver-transmitter handshake procedures are completed, the CRs start receiving and/or transmitting information.

4. Spectrum mobility: CRs must move to other spectrum holes to keep doing communications once they detect the signal from the primary users (PU).

There have been many open research problems to develop these procedures. We can refer to research in [13] which provides an extensive list of current proposals and open challenges for solving above procedures. In Chapter 4, we study the spectrum access/spectrum sharing issues and design a knowledge-based spectrum access scheme to solve the spectrum sharing problem.

1.2 Thesis Organization

The remainder of this thesis is organized as follows. In Chapter 2, the spatial-temporal-frequency diversity to improve the detection performance of Radar Sensor Networks (RSN) in the presence of certain types of interference (clutter, jamming, and interference between radar sensors) and noise is studied. In order to reduce the interference between radar sensors and maximize the signal-to-interference-plus-noise ratio (SINR), we propose a method using the orthogonality criterion to design waveforms for radar sensors in the network. Besides the interference between radar sensors, performance of the network depends largely on other interference, especially clutter, which is extended in both angle and range, and is spread in Doppler frequency. By using the spatial-temporal diversity[1], we can suppress effects of these interference. In this chapter, we also propose a receiver for diversity combining in RSN. As an application example, we apply the spatial-temporal-frequency diversity scheme to improve the detection performance or reduce the miss-detection probability at a low false alarm probability. Simulation results for both non-fluctuating targets and fluctuating targets show that the performance of RSN using our proposed scheme is superior to that of the single radar with the spatial-temporal diversity only.

In many military and civilian applications, estimating the number of targets in a region of interest plays a primary role in performing important tasks such as target

[1]Spatial - Temporal Diversity is also known as Space-Time Adaptive Processing (STAP)

localization, classification, recognition, tracking, etc. Such an estimation problem is, however, very challenging since the number of targets is time-varying, targets' states are fluctuating, and many kinds of targets might appear in the field of interest. Chapter 3 develops a framework for estimating the number of targets in a sensing area using Radar Sensor Networks (RSN): (1) the multi-target detection problem is formulated; (2) signals, interference (e.g., clutter, jamming, and interference between radars) are modeled, and noise at radar sensors; (3) a Maximum Likelihood Multi-Target Detection (ML-MTD) algorithm to combine received measurements and estimate the number of targets present in the sensing area is proposed. We evaluate multi-target detection performance using RSN in terms of the probability of miss-detection P_{MD} and the root mean square error (RMSE). Simulation results show that multi-target detection performance of RSN is much better than that of single radar systems.

Recent studies have shown that, with the traditional spectrum access approach, the radio spectrum assigned to primary (licensed) users (PUs) is vastly underutilized. Amongst proposed methods for using spectrum effectively, the opportunistic spectrum access has become the most viable approach to achieve near-optimal spectrum utilization by allowing secondary (unlicensed) users (SUs) to sense and access available spectrum opportunistically. However, a naive spectrum access for SUs can make spectrum utilization inefficient and increase interference to adjacent users. Chapter 4 proposes a knowledge-based spectrum access scheme to opportunistically control the spectrum access. The spectrum access scheme is built using Fuzzy Logic System (FLS) and spectrum access decision is based on: (1) spectrum utilization efficiency of the secondary user; (2) its degree of mobility; and (3) its average distance to PUs. The output of the FLS provides the probabilities of accessing spectrum band for SUs and the SU with the highest probability will be assigned the available spectrum. We also show that our scheme performs much better than random access approach.

Finally, in Chapter 5, we conclude this thesis and discuss some future research directions on detections in RSN and spectrum access in CSN.

CHAPTER 2

DIVERSITY AND DETECTION IN RADAR SENSOR NETWORKS

2.1 Introduction

Radar sensor networks (RSN) consist of collaboratively operating radar sensors which are deployed ubiquitously (possibly randomly placed) on airborne, surface, and sub-surface unmanned vehicles. Each sensor in the network has capabilities for radar sensing, signal processing, and wireless communication. Autonomous radar sensors operating in the microwave spectrum are used to detect, classify, and track visible, obscured or hidden targets such as tactical weapons, aircraft, ships, spacecraft, vehicles, people, and the natural environment at the presence of both noise and interference (clutter, jamming, and interference between sensors). Information about a target is wirelessly forwarded to the central processor, where target identification and network-wide tracking are conducted using sensor data from every sensor in the network, along with their position and timing information.

In radar sensor networks, radar sensors are networked together in an ad-hoc fashion, i.e., they do not depend on any preexisting infrastructure. They are self-organizing entities that are deployed on demand in support of various events such as surveillance, battlefield, disaster relief, search and rescue, etc. RSN has advantages compared to a single radar system in improving the system sensitivity, reducing obscuration effects and vulnerability, and increasing the detection performance [42], [4]. However, when deploying the RSN, we have to solve some challenging problems such as networking between radar sensors, canceling effects of interference, power efficient communication, reducing complexity of signal processing schemes, etc. Only few work doing research on these aspects has been developed. Recently, S. Kadambe [42] proposed a minimax entropy-based technique to reduce the processing complexity in the RSN. In [4], relative

merits of the RSN and the balance of increased performance, complexity, and cost were discussed. In this chapter, we will examine a method to design the waveform in order to cancel the interference between radar sensors and maximize the signal-to-interference-plus-noise ratio (SINR). In research literature on the waveform design, Fitzgerald [35] demonstrated the inappropriateness of waveform selection based on measurement quality alone: the interaction between the measurement and the track can be indirect, but must be taken into account. Bell [24] used the information theory to design waveform for the measurement of extended radar targets exhibiting resonance phenomena. Baum [3] used the singularity expansion method to design some discriminant waveforms. However, these design methods were used for the single radar only. In [31], radar sensor networks for automatic target recognition were studied, but clutter and jammer were not considered.

Furthermore, the performance of the RSN depends largely on the interference which is extended in both angle and range and is spread in Doppler frequency because of motion of the platform and target. Space-Time Adaptive Processing (STAP) or spatial-temporal diversity has become an excellent technique to suppress effects of interference. STAP refers to the simultaneous processing of the spatial samples from an array antenna and the temporal samples provided by the echoes from multiple pulses of a coherent processing interval (CPI). A considerable amount of work has been done to develop STAP for processing data from airborne or space-borne radars to reliably detect moving targets of interest in the presence of strong clutter returns and jamming [45] [36] [20] [18]. By combining waveform design and spatial-temporal diversity, we can perform spatial-temporal-frequency diversity in RSN. Our studies show that using the proposed diversity scheme can improve the detection performance of RSN with a low false alarm probability.

The remainder of this chapter is organized as follows. In Section 2.2, we examine a method to design waveforms. Spatial-temporal diversity and interference analysis are discussed in Section 2.3 and Section 2.4. In Section 2.5, we propose a diversity combining scheme and analyze detection performance for non-fluctuating targets as well as fluctu-

ating targets using our proposed diversity scheme. Simulation results and performance analysis are discussed in Section 2.6, and in Section 2.7, we conclude the chapter.

2.2 Waveform Design

In radar sensor networks, radar sensors will interfere with one another and SINR will be very low if waveforms are not properly chosen. In order to have waveforms designed properly and coexisted in the network, we use orthogonality as one criterion to design waveforms.

In our study, we choose constant frequency (CF) pulse waveform for radar sensors. The CF waveform can be defined as

$$x(t) = \sqrt{\frac{E}{T}} \exp(j2\pi ft), \qquad 0 \leq t \leq T. \tag{2.1}$$

where E is the energy of the waveform and T is the waveform pulse duration.

We know that the waveforms from different radar sensors will interfere with one another. We choose the waveform for radar i as

$$x_i(t) = \sqrt{\frac{E}{T}} \exp(j2\pi(f + \Delta_i)t), \qquad 0 \leq t \leq T. \tag{2.2}$$

which means that there is a frequency shift Δ_i for the radar sensor i. In order to minimize the interference between radar sensors, we will find a set of frequency shifts $\{\Delta_i\}_{i=0}^{M-1}$ (M is the number of radar sensors) for which the waveforms are orthogonal. Let $R(k,l)$ denote the cross-correlation between the waveforms $x_k(t)$ and $x_l(t)$.

$$\begin{aligned} R(k,l) &= \int_0^T x_k(t)x_l^*(t)dt, \\ &= E\text{sinc}((\Delta_k - \Delta_l)T)\exp(j\pi(\Delta_k - \Delta_l)T). \end{aligned} \tag{2.3}$$

where a superscript asterisk indicates the complex conjugate. If $\pi(\Delta_k - \Delta_l)T = i\pi$, the waveforms $x_k(t)$ and $x_l(t)$ are orthogonal, i.e.,

$$R(k,l) = \begin{cases} 0 & k \neq l \\ E & k = l \end{cases}$$

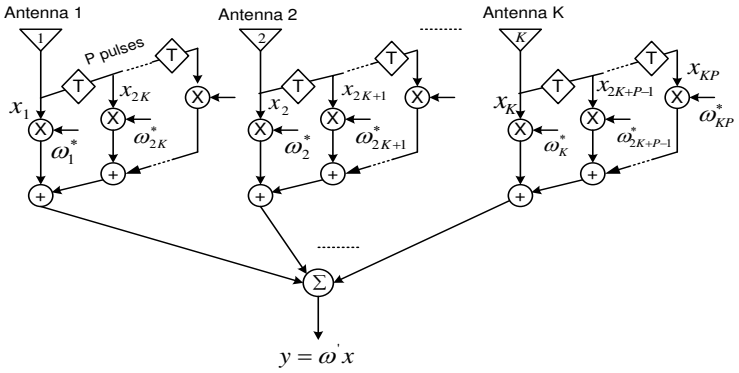

Figure 2.1: Space-time beamformer consisting of an K-element ULA and a coherent processing interval (CPI) comprising P pulses with a fixed PRI [18]

Therefore, we can choose a set of frequency shifts $\{\Delta_i\}_{i=0}^{M-1}$ as below [31]:

$$\Delta_i = \Delta_k - \Delta_l = \frac{i}{T}, \qquad i = 0,\ 1,\ ...,\ M-1. \tag{2.4}$$

Based on (2.4), we can confirm that the waveforms can co-exist if the frequency shift is i/T between two waveforms, i.e., orthogonality among waveforms can be achieved by separating frequencies of waveforms by multiplying an integer with the inverse of the waveform pulse duration. So, we will choose the waveforms by this method to get radar sensors coexisted in RSN. Moreover, by using this waveform design method, we can perform a frequency diversity in RSN.

2.3 Spatial - Temporal Diversity

At radar sensor i, we use a receiver with an array antenna as shown in Fig. 2.1. This array consists of an K-element ULA with inter-element spacing d_i (spatial degrees of freedom) and P pulse repetition interval (PRI) time taps (temporal degrees of freedom).

Now, we consider a signal $g_i(t) = A\exp(j2\pi f_i t)$ at a frequency f_i impinging on the array. If the wave's angle of arrival relative to the array is φ_i, the signal observed at the kth array element is

$$s_k(t) = A\exp\{j(2\pi f_i(t - kd_i\sin\varphi_i/c) + \phi_0)\}, \quad k = 0,\ 1,\ ...,\ K-1. \tag{2.5}$$

where the phase offset ϕ_0 accounts for the absolute phase at the first element. We consider K samples formed from K array elements at a time t_0 and map these K element samples into a vector form to have a snapshot of the array at a fixed time.

$$\begin{aligned} \mathbf{s} &= A_1[1 \quad \exp(-j2\pi d_i \sin\varphi_i/\lambda_i) \quad ... \quad \exp(-j2\pi(K-1)d_i \sin\varphi_i/\lambda_i)]', \\ &= A_1\mathbf{a}_s(\theta_i). \end{aligned} \tag{2.6}$$

where $(.)'$ denotes the transpose operation, $A_1 = A\exp(j(2\pi f_i t + \phi_0))$, $\theta_i = d_i \sin\varphi_i/\lambda_i$ is the normalized angle, and $\mathbf{a}_s(\theta_i)$ is the spatial steering vector.

$$\mathbf{a}_s(\theta_i) = [1 \quad \exp(-j2\pi\theta_i) \quad ... \quad \exp(-j2\pi(K-1)\theta_i)]'. \tag{2.7}$$

Since the target is in motion, the normalized Doppler shift at the target induced on the radar sensor i at an angle φ_i is

$$f_i = \frac{2v_i T}{\lambda_i}\sin\varphi_i = \beta\theta_i. \tag{2.8}$$

where v_i is the velocity of the radar sensor i and $\beta = \frac{2v_iT}{d_i} = \frac{4v_iT}{\lambda_i}\,|_{d_i=\frac{\lambda_i}{2}}$. Each vector of array outputs from successive pulses due to the target will have a temporal linear phase progression. Therefore, at the pth PRI, snapshot of the target takes the form [18], [22]:

$$\mathbf{e}(\theta_i, f_i) = \exp(j2\pi(p-1)f_i)\mathbf{a}_s(\theta_i), \qquad p = 1, 2, ..., P. \tag{2.9}$$

If P pulses are to be processed in a coherent pulse interval (CPI), the KP dimensional space-time steering vector (snapshot) corresponding to a possible target at look angle φ_i and Doppler frequency f_i is given by

$$\mathbf{e}(\theta_i, f_i) = \mathbf{b}_t(f_i) \otimes \mathbf{a}_s(\theta_i). \tag{2.10}$$

where $\otimes$ denotes the Kronecker product[1] and $\mathbf{b}_t(f_i)$ is the P-dimensional Doppler steering vector.

$$\mathbf{b}_t(f_i) = [1 \quad \exp(j2\pi f_i) \quad ... \quad \exp(j2\pi(P-1)f_i)]'. \tag{2.11}$$

[1]In mathematics, the Kronecker product, denoted by $\otimes$, is an operation on two matrices of arbitrary size resulting in a block matrix. If $\mathbf{A}$ is an m-by-n matrix and $\mathbf{B}$ is a p-by-q matrix, then the Kronecker product $\mathbf{A} \otimes \mathbf{B}$ is the mp-by-nq block matrix.

By introducing the complex weighting vector ω_i, the output response of the space-time beamformer can be maximized for any desired angle of arrival. More specifically, let $\mathbf{x}_i$ and y_i denote the received data at radar sensor i and beamformer output, respectively.

$$y_i = \omega_i' \mathbf{x}_i. \tag{2.12}$$

In any case, the optimum weight vector, $\omega_i \in \mathcal{C}^{KP}$, that maximizes SINR, satisfies the Weiner-Hopf equation:

$$\omega_i = \mathbf{R}_i^{-1} \mathbf{e}(\theta_i, f_i). \tag{2.13}$$

where $\mathbf{R}_i \in \mathcal{C}^{KP \times KP}$ is the interference-plus-noise covariance matrix.

In practice, the covariance matrix $\mathbf{R}_i$ is unknown and must be estimated; and determining ω_i is a challenging problem. To solve this problem, researchers have produced extensively algorithms [38] [11] [15] [44] to choose an optimal set of complex space-time weights ω_i in order to maximize SINR.

2.4 Interference and Noise Analysis

2.4.1 Clutter

Clutters generate unwanted radar returns that may interfere with the desired signal. Parasitic returns that enter the radar through the antenna's main-lobe are called main-lobe clutter; otherwise, they are called side-lobe clutter. Clutter can be classified into two main categories: surface clutter (including trees, vegetation, ground terrain, man-made structures, and sea surface) and volume clutter (including chaff, rain, birds, and insects). Surface clutter changes from one area to another, while volume clutter may be predictable. In many scenarios, the dominant disturbance in radar networks is not noise, but clutter. Consequently, the signal-to-clutter ratio (SCR) is often more important than the signal-to-noise ratio (SNR).

The integrated clutter can be generally approximated as the sum of N_{ci} clutter patches. For clutter patch k, the space-time data vector is modeled as [18]

$$\begin{aligned} \mathbf{p}_{ki} &= \xi_{ki}\mathbf{b}_t(f_{ki}) \otimes \mathbf{a}_s(\theta_{ki}) \\ &= \xi_{ki}\mathbf{u}_{ki}, \quad k = 1, 2, ..., N_{ci}. \end{aligned} \tag{2.14}$$

where ξ_{ki} is a complex random variable that accounts for the amplitude and phase of clutter patch k. $\mathbf{u}_{ki} = \mathbf{b}_t(f_{ki}) \otimes \mathbf{a}_s(\theta_{ki})$ where $\mathbf{b}_t(f_{ki})$ and $\mathbf{a}_s(\theta_{ki})$ are temporal vector and spatial vector of clutter patch k, respectively. f_{ki} and θ_{ki} are the normalized Doppler shift and angle of arrival of the kth clutter patch, respectively. Total clutter vector $\mathbf{w}_{ci}$ equals to

$$\begin{aligned} \mathbf{w}_{ci} &= \sum_{k=1}^{N_{ci}} \xi_{ki}\mathbf{b}_t(f_{ki}) \otimes \mathbf{a}_s(\theta_{ki}) \\ &= \sum_{k=1}^{N_{ci}} \xi_{ki}\mathbf{u}_{ki}. \end{aligned} \tag{2.15}$$

The $KP \times KP$ covariance matrix of the clutter $\mathbf{R}_{ci}$ at the ith radar is given by

$$\begin{aligned} \mathbf{R}_{ci} &= E\{\mathbf{w}_{ci}\mathbf{w}_{ci}^H\} \\ &= \sum_{k=1}^{N_{ci}}\sum_{j=1}^{N_{ci}} E\{\xi_i\xi_j^H\}\mathbf{u}_{ki}\mathbf{u}_{ji}^H, \\ &= \sigma_{ci}^2\mathbf{M}_{ci}. \end{aligned} \tag{2.16}$$

where H denotes the Hermitian operation, $E\{\cdot\}$ denotes the expectation, and $\mathbf{M}_{ci}$ is the normalized covariance matrix, i.e., all diagonal entries of $\mathbf{M}_{ci}$ are ones.

2.4.2 Jamming

Jamming signals are generated by hostile interfering signal sources that seek to degrade the performance of radar sensors by mechanisms such as degrading signal-to-interference-plus-noise ratio (SINR) by increasing the noise level, or generating false

detections to overwhelm RSN with false targets. A model for N_{ji} jamming signals is commonly presented as [45]

$$\mathbf{w}_{ji} = \sum_{l=1}^{N_{ji}} \beta_l \otimes a_{ji}(\theta_l), \quad i = 1, 2, ..., N. \tag{2.17}$$

where β_l contains voltage samples of the lth jammer waveform and $a_{ji}(\theta_l)$ is the jamming signal waveform at an angle θ_l. The different jamming waveforms are uncorrelated with each other.

2.4.3 Interference between Radar Sensors

When we deploy the radar sensor network, waveforms from different radar sensors will interfere with each other. Thus, interference between radar sensors need to be studied. Interference between radar sensors was analyzed in [31]. To suppress this interference, we should choose waveforms correctly. Based on [31], we choose the orthogonality criterion to design the waveforms.

2.4.4 Thermal Noise

The echo signal received from a target or clutter inevitably competes with noise. Noise can be received through antenna from external sources or generated in the radar receiver itself. Among noise existing in RSN, thermal noise due to ohmic losses at the radar receiver is normally dominant. We model the thermal noise vector $\mathbf{n}_i$ at radar sensor i as a complex white Gaussian vector with zero-mean and covariance σ_{ni}^2. The covariance matrix of noise $\mathbf{R}_{ni} = \sigma_{ni}^2\mathbf{I}$ where $\mathbf{I}$ is the $KP \times KP$ identity matrix.

2.5 Diversity Combining and Target Detection

Radar sensor networks are composed of many radar sensors deployed in a large geographical area. Radar sensors (nodes) are networked together in an ad-hoc fashion, i.e., they do not depend on any preexisting infrastructure. In fact, they are self-organizing entities that are deployed on demand to perform various tasks such as surveillance, disas-

ter relief, search and rescue, etc. Scalability concerns suggest a hierarchical organization of the radar sensor networks with the lowest level in the hierarchy being a cluster. The clusters are independently controlled and dynamically reconfigured as nodes move. Thus, this network architecture has some main advantages as follows [5]

1. Using the radio resources efficiently. For example, bandwidth can be shared or reserved in a controlled fashion in each cluster.
2. Providing spatial and frequency reuse due to node clustering.
3. Robustness with topological changes caused by node motion, node failure, and node insertion/removal.
4. Concealing the details of global network topology from individual nodes.

In our work, each sensor in the network will be assigned a waveform with specific parameters. Radar sensors can provide their parameters about waveforms to the cluster-head where waveforms from cluster members are collected and combined.

The received data at radar sensor i consists of the desired signal and disturbance which includes interference and noise, i.e.,

$$\mathbf{x}_i(u,t) = \alpha_i(u)\mathbf{e}(\theta_i, f_i)s_i(t-\tau_i) + \mathbf{w}_i + \mathbf{n}_i. \tag{2.18}$$

$$\mathbf{w}_i = \mathbf{w}_{ci} + \mathbf{w}_{ji} + \mathbf{w}_{ri}. \tag{2.19}$$

where $\mathbf{w}_i$ presents the overall interference which is the sum of the clutter vector $\mathbf{w}_{ci}$, the jamming vector $\mathbf{w}_{ji}$, and the interference between radar sensors $\mathbf{w}_{ri}$. $\mathbf{n}_i$ is the background white noise. $\alpha_i(u)$ is a random variable that models the radar cross section (RCS), $\mathbf{e}(\theta_i, f_i)$ is a spatial-temporal steering vector that models the target return with an angle θ_i and a Doppler shift f_i, and $s_i(t-\tau_i)$ is the return of waveform with delay τ_i.

The data at the output of the ith sensor is the multiplication of the received data $\mathbf{x}_i(u,t)$ and the spatial-temporal weight vector ω_i, i.e.,

$$\begin{aligned} y_i(u,t) &= \omega_i^{'}\mathbf{x}_i(u,t), \\ &= \omega_i^{'}[\alpha_i(u)\mathbf{e}(\theta_i, f_i)s_i(t-\tau_i) + \mathbf{w}_i + \mathbf{n}_i], \\ &= \alpha_i(u)s_i(t-\tau_i)L_i(\theta_i, f_i) + D_i. \end{aligned} \tag{2.20}$$

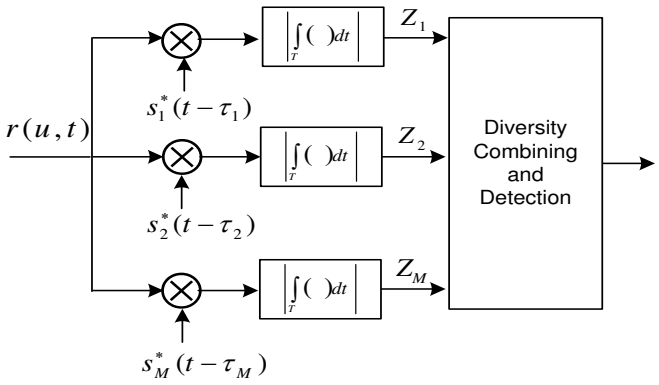

Figure 2.2: Structure of the receiver at the clusterhead for diversity combining

where $D_i \triangleq \omega_i'(\mathbf{w}_i + \mathbf{n}_i)$ and $L_i(\theta_i, f_i) \triangleq \omega_i'\mathbf{e}(\theta_i, f_i)$.

Assume that the radar sensor network consists of M radar sensors, the received signal $r(u,t)$ at the cluster-head is

$$\begin{aligned} r(u,t) &= \sum_{i=1}^{M} y_i(u,t), \\ &= \sum_{i=1}^{M} \{\alpha_i(u) s_i(t-\tau_i) L_i(\theta_i, f_i) + D_i\}. \end{aligned} \tag{2.21}$$

Note that $\alpha_i(u)$ can be modeled using non-zero constants, e.g., Swerling target models 0 or V, for non-fluctuating targets and random variables, e.g., Swerling target models I-IV, for fluctuating targets. Target fluctuation might lower the probability of detection or equivalently reduce SINR [29].

At the cluster-head, we use a receiver proposed in [31] to combine waveforms. The structure of receiver is shown in the Fig. 2.2. According to this receiver, the received signal $r(u,t)$ is processed by a bank of matched filters. After integration, the output of the branch 1 is given by

$$Z_1(u) = |\int_0^T r(u,t) s_1^*(t-\tau_1) dt|, \tag{2.22}$$

$$\begin{aligned} &= |\sum_{i=1}^{M} \alpha_i(u) L_i(\theta_i, f_i) \int_0^T s_i(t-\tau_i) s_1^*(t-\tau_1) dt + \sum_{i=1}^{M} \int_0^T s_1^*(t-\tau_1) D_i dt|, \\ &= |Z_{11}(u) + Z_{12}(u)|. \end{aligned} \tag{2.23}$$

where $Z_{11}(u)$ and $Z_{12}(u)$ are defined as below

$$\begin{aligned} Z_{11}(u) &\triangleq \sum_{i=1}^{M} \alpha_i(u) L_i(\theta_i, f_i) \int_0^T s_i(t-\tau_i) s_1^*(t-\tau_1) dt, \quad (2.24) \\ &= \sum_{i=2}^{M} \alpha_i(u) L_i(\theta_i, f_i) \int_0^T s_i(t-\tau_i) s_1^*(t-\tau_1) dt + E\alpha_1(u) L_1(\theta_1, f_1). \\ Z_{12}(u) &\triangleq \sum_{i=1}^{M} \int_0^T s_1^*(t-\tau_1) D_i dt. \quad (2.25) \end{aligned}$$

Based on (2.4), $Z_{11}(u)$ can be rewritten as

$$Z_{11}(u) = E\alpha_1(u) L_1(\theta_1, f_1). \quad (2.26)$$

Assuming that waveforms are designed properly. So the interference between radar sensors is negligible. Since the detection performance of RSN is greatly affected by the clutter, we consider the clutter the primary interference source. The overall disturbance is the sum of clutter and noise. That is,

$$\begin{aligned} \mathbf{w}_i &= \mathbf{w}_{ci} + \mathbf{n}_i, \quad (2.27) \\ &= \sum_{j=1}^{N_c} \gamma_{ij} \mathbf{u}_{ij} + \mathbf{n}_i. \quad (2.28) \end{aligned}$$

where $\mathbf{u}_{ij} = \mathbf{b}_t(f_{ki}) \otimes \mathbf{a}_s(\theta_{ki})$. Thus, $Z_{12}(u)$ becomes

$$Z_{12}(u) = \sum_{i=1}^{M} \int_0^T \omega_i^{'} \mathbf{w}_i s_1^*(t-\tau_1) dt. \quad (2.29)$$

Since γ_{ij} is a complex random variable, we assume γ_{ij} is a complex Gaussian random variable. Therefore, it is not difficult to prove that Z_{12} is a complex Gaussian noise $n(u)$. Then, the output of the branch 1 becomes

$$Z_1(u) \approx |E\alpha_1(u) L_1(\theta_1, f_1) + n(u)|. \quad (2.30)$$

Similarly, the output of the ith branch ($i = 1, 2, ..., M$) can be written as

$$Z_i(u) \approx |E\alpha_i(u) L_i(\theta_i, f_i) + n(u)|. \quad (2.31)$$

Based on (2.31), we can recognize that the output of the ith branch is composed of the signal from the radar sensor i and noise. Note that when we compute $Z_i(u)$, we still have to estimate the interference-plus-noise covariance matrix.

Our objective is now to combine the outputs of all branches and use the spatial-temporal-frequency diversity to improve the target detection performance of RSN. We know that the purpose of detection problem is to figure out the presence or absence of the desired targets such as missiles, tanks, fighter aircrafts, other tactical weapons from the enemy, illegal intruders at the border of the country, over-speeded vehicles or strange ships at sea, etc. In this work, we use an equal gain combining method to combine the outputs of all branches and apply a Neyman-Pearson criterion to detect the presence/absence of targets. To analyze the detection performance of RSN for both non-fluctuating targets and fluctuating targets, we use miss-detection probability and false alarm probability as evaluation metrics. The detection problem in RSN can be formulated as a binary hypothesis testing problem. We define two hypotheses H_0 and H_1 as follows:

$$\begin{aligned} H_0 &: \text{Target is not present} \\ H_1 &: \text{Target is present} \end{aligned} \tag{2.32}$$

2.5.1 Non-fluctuating Targets

Non-fluctuating targets can be modeled as the Swerling 0 or equivalently Swerling V [1], [29]. The radar cross section (RCS) $\alpha_i(u)$ of non-fluctuating targets is constant and unknown. We assume that RCS of the target at radar sensors is similar. That is,

$$\alpha_1(u) = \alpha_2(u) = ... = \alpha_M(u) = \alpha(u). \tag{2.33}$$

Under hypothesis H_0, $Z_i(u)$ follows the Rayleigh distribution. Therefore, the probability density function (pdf) of Z_i is

$$f(z_i|H_0) = \frac{2z_i}{\sigma^2}\exp(-\frac{z_i^2}{\sigma^2}). \tag{2.34}$$

Under hypothesis H_1, $Z_i(u)$ follows the Rician distribution. So the pdf of Z_i with the parameter m_i is

$$f(z_i|H_1) = \frac{2z_i}{\sigma^2}\exp(-\frac{z_i^2+m_i^2}{\sigma^2})I_0(\frac{2m_iz_i}{\sigma^2}). \tag{2.35}$$

where $m_i = E\alpha(u)L_i(\theta_i, f_i)$, $\sigma^2/2$ is the noise power for each branch I, Q, and $I_0(.)$ is the zero-order modified Bessel function of the first kind. We assume that $Z_1, Z_2, ..., Z_m$ are independent random variables. Let $Z \stackrel{\triangle}{=} (Z_1, Z_2, ..., Z_M)$, the joint pdf of the variable Z for each hypothesis:

$$f(z|H_0) = \prod_{i=1}^{M}\frac{2z_i}{\sigma^2}\exp(-\frac{z_i^2}{\sigma^2}). \tag{2.36}$$

$$f(z|H_1) = \prod_{i=1}^{M}\frac{2z_i}{\sigma^2}\exp(-\frac{z_i^2+m_i^2}{\sigma^2})I_0(\frac{2m_iz_i}{\sigma^2}). \tag{2.37}$$

2.5.2 Fluctuating Targets

In practice, RCS is normally fluctuating. Based on different combinations of pdf and decorrelation (pulse to pulse or scan to scan), Swerling [29] proposed four Swerling models which are Swerling models I-IV to model RCS for fluctuating targets. He showed that the statistics associated with Swerling I and II models are applied to targets consisting of many small RCS scatters of comparable RCS values, while the statistics associated with Swerling III and IV models are applied to targets consisting of one large scatter and many small equal RCS scatters [1].

In our work, we focus our studies on the Swerling II model. The magnitude $|\alpha(u)|$ of Swerling II targets fluctuates independently from pulse to pulse according to a chi-square probability density function with two degree of freedom, i.e., a Rayleigh probability density function.

$$\alpha(u) = \alpha_I(u) + j\alpha_Q(u). \tag{2.38}$$

where $\alpha_I(u)$ and $\alpha_Q(u)$ follow Gaussian distribution with the variance $\rho^2/2$ for each branch I, Q. Under hypothesis H_0, $Z_i(u)$ follows the Rayleigh distribution. Hence, the pdf of $Z_i(u)$ is

$$f(z_i|H_0) = \frac{2z_i}{\sigma^2}\exp(-\frac{z_i^2}{\sigma^2}). \tag{2.39}$$

Under hypothesis H_1, $Z_i(u)$ follows the Rayleigh distribution. Thus the pdf of $Z_i(u)$ is given as

$$f(z_i|H_1) = \frac{2z_i}{\sigma_i^2}\exp(-\frac{z_i^2}{\sigma_i^2}). \tag{2.40}$$

where $\sigma_i = \sqrt{(EL_i(\theta_i, f_i))^2\rho^2 + \sigma^2}$. We assume that $Z_1, Z_2, ..., Z_m$ are independent random variables. Let $Z \stackrel{\triangle}{=} (Z_1, Z_2, ..., Z_M)$, the joint pdf of the variable Z for each hypothesis:

$$f(z|H_0) = \prod_{i=1}^{M}\frac{2z_i}{\sigma^2}\exp(-\frac{z_i^2}{\sigma^2}). \tag{2.41}$$

$$f(z|H_1) = \prod_{i=1}^{M}\frac{2z_i}{\sigma_i^2}\exp(-\frac{z_i^2}{\sigma_i^2}). \tag{2.42}$$

For both non-fluctuating and fluctuating targets, our objective is to decide whether or not a target is present based on the received signal at the cluster-head. The likelihood ratio is computed as:

$$\Lambda = \frac{f(z|H_1)}{f(z|H_0)}. \tag{2.43}$$

We assume that the probability of presence of a target is equal to the probability of absence of a target. This means that $P(H_1) = P(H_2)$. Therefore, using the Neyman-Pearson criterion, our detection problem can be simplified as

- If $\Lambda > \nu$ where ν is a detection threshold, then we claim that the target is present.
- If $\Lambda < \nu$, then we claim that the target is absent.

To evaluate detection performance, we use the false alarm probability P_{FA} and miss-detection probability P_{MD}. According to [43], we can constrain P_{FA} by choosing the threshold ν. P_{MD} and P_{FA} are defined:

$$\begin{aligned} P_{MD} &= P(H_0|H_1), \\ &= P(\Lambda < \nu|H_1). \end{aligned} \tag{2.44}$$

$$\begin{aligned} P_{FA} &= P(H_1|H_0), \\ &= P(\Lambda > \nu|H_0). \end{aligned} \tag{2.45}$$

2.6 Simulation Results and Detection Performance Analysis

2.6.1 Simulated Data Model

In this work, we use the modified Joint Domain Localized (JDL) algorithm proposed by Adve *et.al* [38] to determine the space-time weights at sensors. The data generation scheme uses the physical model presented by Ward [20].

As mentioned in the section 2.3, the clutter is modeled as a sum of the contributions of many discrete far field sources. We assume that amplitude of each discrete source is a complex Gaussian random variable whose average power is set by a chosen clutter-to-noise ratio (CNR). The normalized Doppler shift associated with each clutter source depends on the velocity of the platform.

Thermal noise is modeled as a Gaussian white noise process. The average power is set to unity, allowing the clutter and target powers to be referenced to the white noise power. Simulations do not consider the effects of Jammers. Parameters used in simulations are listed in the Table 2.1 [38].

Table 2.1: Parameters used in simulations

Parameters	Values
Array elements	8
Pulses	8
Element spacing	$\lambda_i/2$
Pulse Repetition Frequency (PRF)	1024 Hz
The number of clutter sources	181
Thermal noise power	Unity
Clutter to noise ratio (CNR)	50 dB
The number of Doppler bins in LPR	3
The number of Angle bins in LPR	3

Suppose that the interference-plus-noise covariance matrices at radar sensors are similar. This mean that $\mathbf{R}_{d1} = \mathbf{R}_{d2} = ... = \mathbf{R}_{dM} = \mathbf{R}_d$. $\mathbf{R}_d$ is computed by

$$\mathbf{R}_d = \mathbf{R}_n + \varepsilon_c(h)\mathbf{R}_c \tag{2.46}$$

where $\mathbf{R}_n$ is the covariance matrix of noise, $\mathbf{R}_c$ is the clutter covariance matrix, and $\varepsilon_c(h)$ is a random variable used to model the clutter power of the hth range cell. $\varepsilon_c(h)$ often follows Weibull or gamma distribution [37][46]. In homogeneous environments, the average clutter power does not depend on h. Consequently, our objective is to evaluate the detection gain when radar sensors are networked.

2.6.2 Detection Performance Analysis

In RSN, each radar sensor transmits a known waveform. This waveform is then reflected back from the target toward the receiving sensor. RSN's tasks are to detect the existence of the target and to estimate its unknown parameters, e.g., range speed and direction. In our work, we use the spatial-temporal-frequency diversity in RSN to improve the detection performance. To evaluate detection performance, we investigate two types of targets such as non-fluctuating targets and fluctuating targets. Fig. 2.3a presents the probability of miss-detection P_{MD} as a function of signal-to-clutter-plus-noise ratio (SCNR) and $P_{FA} = 10^{-6}$ while Fig. 2.3b presents the miss-detection probability P_{MD} as the function of false alarm probability P_{FA} and SCNR = 10 dB for non-fluctuating targets. Similarly, Fig. 2.4a presents the probability of miss-detection P_{MD} as a function of SCNR and $P_{FA} = 10^{-6}$ while Fig. 2.4b presents the miss-detection probability P_{MD} as the function of false alarm probability P_{FA} and SCNR = 10 dB for fluctuating targets.

Based on results in Fig. 2.3 and Fig. 2.4, we recognize that the probability of miss-detection P_{MD} is extremely reduced when the number of radar sensors increases. For instance, at the same SCNR = 10 dB, P_{MD} of the 2-radar RSN is lower than that of the single radar system. For non-fluctuating targets, P_{MD} of the 2-radar RSN and the single radar system is greater than 10%, while P_{MD} of the 5-radar RSN is much lower than 10%.

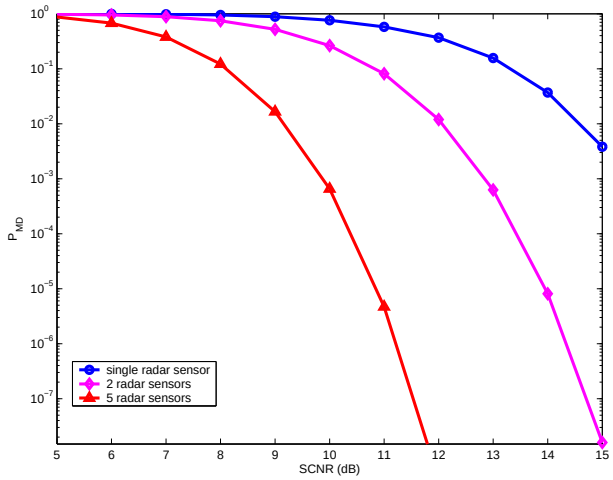

(a)

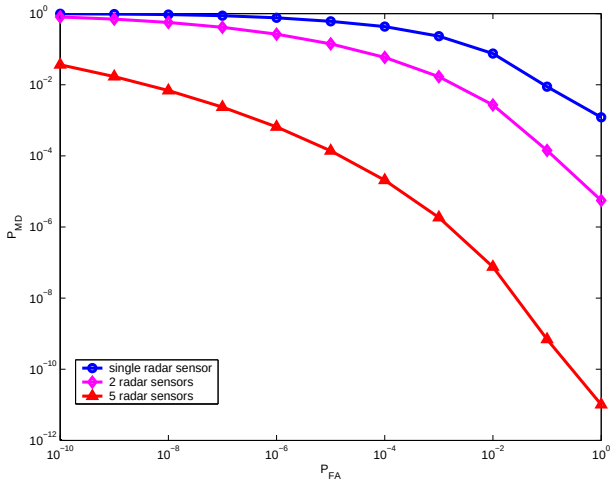

(b)

Figure 2.3: Non-fluctuating target models: (a) Miss-detection probability P_{MD} as a function of SCNR, $P_{FA} = 10^{-6}$, (b) Miss-detection probability P_{MD} as the function of false alarm probability P_{FA}, SCNR=10 dB

However, for fluctuating targets, P_{MD} of the 2-radar RSN and the single radar system is much greater than 10%, while P_{MD} of the 5-radar RSN is a little lower than 10%. It is desirable for P_{MD} to be as low as possible. In the real world, P_{MD} less than 10% is reasonable [14]. For both target types, we can observe that it is very difficult to achieve this reasonable P_{MD} with the single radar system at a low P_{FA}; and if possible, the SCNR must be larger than 14 dB for non-fluctuating targets and 21 dB for fluctuating targets. In case we use the 2-radar RSN; we can achieve the P_{FA}=10% with SCNR around 8 dB

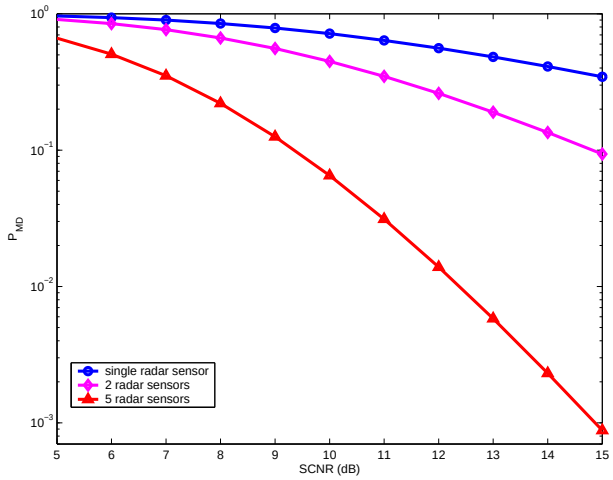

(a)

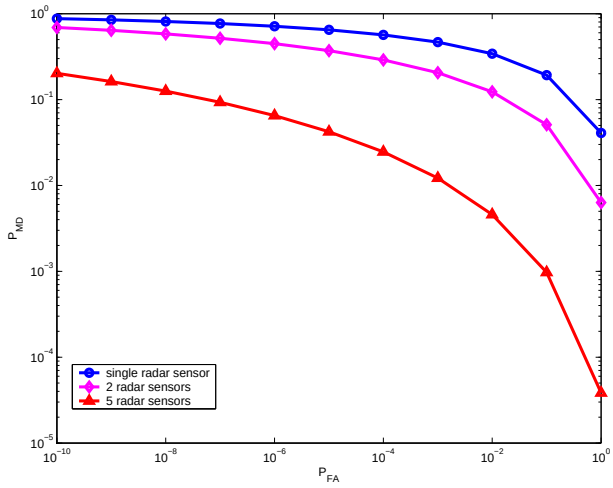

(b)

Figure 2.4: Fluctuating target models: (a) Miss-detection probability of miss-detection P_{MD} as a function of SCNR, $P_{FA} = 10^{-6}$, (b) Miss-detection probability P_{MD} as the function of false alarm probability P_{FA}, SCNR=10 dB

for non-fluctuating targets and around 15 dB for fluctuating targets. Nevertheless, the 5-radar RSN can maintain very low P_{MD} at a low SCNR.

We also notice that it requires more SCNR with fluctuating targets than that with non-fluctuating targets to achieve the same P_{MD}. For example, when we use 5 radar sensors and P_{MD} is about 10%, SCNR is 9.3 dB for fluctuating targets but less than 9 dB for non-fluctuating targets. Furthermore, Fig. 2.3b and Fig. 2.4b show that, at the same values of P_{MD} and SCNR, P_{FA} for non-fluctuating targets is lower than for

fluctuating targets. So depending on specific scenarios, we can choose P_{FA} and SCNR logically in order to get the desired detection performance.

2.7 Conclusions

In this chapter, we investigated and applied the spatial-temporal-frequency diversity to improve the detection performance of RSN. We also proposed a receiver for diversity combining in RSN. The probability of miss-detection as a function of the false alarm probability and the signal-to-clutter-plus-noise (SCNR) is analyzed for both non-fluctuating targets and fluctuating targets. Simulation results showed that the detection performance of our diversity scheme-based radar sensor networks is much better than that of single radar systems using the spatial-temporal diversity only.

CHAPTER 3

COLLABORATIVE MULTI-TARGET DETECTION IN RADAR SENSOR NETWORKS

3.1 Introduction and Motivations

Radar sensor networks (RSN) are networks of distributed radar sensors which collaboratively operate and are deployed ubiquitously on airborne, surface, and unmanned vehicles in a large geographical area. Radar sensors have capabilities for radar sensing, signal processing, and wireless communications. In RSN, radar sensors are networked together in an ad-hoc fashion, i.e., they do not depend on any preexisting infrastructure. In fact, they are self-organizing entities that are deployed on demand to perform various tasks such as surveillance, search and rescue, disaster relief, etc. RSN have advantages compared to single radar systems in improving the system sensitivity, reducing obscuration effects and vulnerability, and increasing the detection performance [42], [4].

An RSN is organized into clusters, which are independently controlled and dynamically reconfigured as sensors move, to observe targets such as tactical weapons, missiles, aircraft, ships, etc. in the surveillance area. In a cluster, sensors receive the signals backscattered by targets in the presence of interference (e.g., clutter, jamming, interference between radar sensors) and noise. Then, the observed signals from all radar sensors are forwarded to a clusterhead where received data set will be combined to perform fundamental tasks such as detection, localization, identification, classification, and tracking. For target detection problem, there are two primary levels: single target detection and multi-target detection. In the single target scenario, we proposed a diversity scheme in Chapter 2 and [9] to improve detection performance of RSN in the presence of strong interference, especially clutters, and noise. We are now interested in using RSN to estimate the number of targets present in the surveillance area. In practice, multiple moving

targets might appear in the sensing area, the number of targets is time-varying, and targets' states are fluctuating. Therefore, the multi-target detection is more challenging and difficult to solve than the single target detection.

Among the existing work on multi-target detection, Yung and Mourad [49] used frequency diversity signaling to estimate the number of moving targets. Kaveh *et al.* [26] applied the information theoretic criteria to detect the number of targets. However, both works only studied the performance of their proposals for the case of two closely spaced targets. A performance analysis for a general case was provided in [47] and [33]. In [6], multiple target detection and estimation by exploiting the amplitude modulation induced by antenna scanning was proposed and a sequential hypothesis test was examined to determine the number of targets. However, all above work studied multi-target detection problem using a single radar. For the sensor network scenario, Wang *et al.* [48] applied Bayesian source number estimation to solve the distributed multiple target detection in sensor networks. Based on their approach, each cluster computed the posterior probability corresponding to each hypothesis on the number of sources and a central processor fused posterior probabilities using Bayes' theorem to select the best hypothesis. Their proposal however did not consider Doppler shifts of the targets and was not suitable for the multi-target detection in RSN.

In this chapter, we develop a framework for estimating the number of targets in the field of interest using RSN. At the ith sensor, we deploy a receiver with an K element-ULA (Uniform Linear Array) whose spacing between elements is d_i. During the observation time, P pulses are transmitted to track targets. The useful signals backscattered from targets include spatial-temporal snapshots of targets and parameters representing radar cross section of targets. Then, a RSN-clusterhead collects measurements from all radar sensors and combines them to perform detection procedures. To fuse received measurements and estimate the unknown number of targets in the area of interest, at the RSN-clusterhead, we propose a multi-target detection algorithm which is Maximum Likelihood Multi-Target Detection (ML-MTD) algorithm. We use the probability of miss-detection

P_{MD} and the root mean square error (RMSE) as metrics to evaluate multi-target detection performance using RSN. Simulation results show that detection performance of the RSN is much better than that of a single radar system.

The rest of this chapter is organized as follows. In Section 3.2, we state our multi-target detection problem. In Section 3.3 and In Section 3.4, we model signals, interference, and noise at radar sensors. In Section 3.5, we propose an ML-MTD algorithm to estimate the number of targets present in the sensing field. Multi-target detection performance of RSN is discussed in Section 3.6 while conclusions and open directions are given in Section 3.7.

3.2 Multi-Target Detection Problem Statement

In this work, we address a realistic situation in which the number of targets to be detected is generally unknown and has to be estimated. To handle our problem, an RSN consisting of N radar sensors is deployed. Radar sensors receive signals embedded in interference and forward them to a central processor, e.g., a clusterhead to perform detection tasks. At the RSN-clusterhead, we propose a detection algorithm to estimate the number of targets. To support the rest of the paper, we make some assumptions as follows:

- Targets evolve along independent trajectories and do not leave the surveillance area during the entire observation time of P consecutive pulses.
- Targets are modeled as Swerling II target models whose magnitudes fluctuate independently from pulse to pulse according to a chi-square probability density function.
- The locations of targets are unknown. Besides, Doppler frequencies when targets are moving relatively to radar platforms are uncertain.
- Observation data or measurements from radar sensors, at the RSN-clusterhead, are statistically independent. The measurements furthermore either originate from true targets or clutters.

The estimated number of targets present in the surveillance area is determined as

$$\{\hat{\tau}_1, \hat{\tau}_2, ..., \hat{\tau}_N\} = \arg \min_{\tau_1, \tau_2, ..., \tau_N} \Lambda(\tau). \tag{3.1}$$

where $\hat{\tau}_i$ is the estimated number of targets at sensor i and $\Lambda(\tau)$ is an utility function derived in 3.5. Hence, the possible number of targets $\widehat{M}$ that RSN can detect is the average value of $\hat{\tau}_1, \hat{\tau}_2, ...,$ and $\hat{\tau}_N$, i.e.,

$$\widehat{M} = \lceil \frac{1}{N} \sum_{i=1}^{N} \hat{\tau}_i \rceil. \tag{3.2}$$

where $\lceil \cdot \rceil$ denotes a ceil operation.

3.3 Signal Model

At radar sensor i, we deploy a receiver with an K-element ULA whose spacing between elements is d_i. If P pulses are processed in a coherent pulse interval, the snapshot of target m is a $KP \times 1$ spatial-temporal steering vector with the following form [45], [18]:

$$\mathbf{e}(\theta_{im}, f_{im}) = \mathbf{b}_t(f_{im}) \otimes \mathbf{a}_s(\theta_{im}). \tag{3.3}$$

where f_{im} and θ_{im} are the normalized Doppler shift and normalized angle for the target m, respectively. The notation $\otimes$ denotes the Kronecker product, $\mathbf{b}_t(f_{im})$ is a $P \times 1$ Doppler steering vector, and $\mathbf{a}_s(\theta_{im})$ is a $K \times 1$ spatial steering vector. $\mathbf{b}_t(f_{im})$ and $\mathbf{a}_s(\theta_{im})$ are defined as follows:

$$\mathbf{b}_t(f_{im}) = [1 \quad e^{j2\pi f_{im}} \quad ... \quad e^{j2\pi(P-1)f_{im}}]^T. \tag{3.4}$$

$$\mathbf{a}_s(\theta_{im}) = [1 \quad e^{-j2\pi\theta_{im}} \quad ... \quad e^{-j2\pi(K-1)\theta_{im}}]^T. \tag{3.5}$$

where T denotes the transpose operation. Let ϕ_{im} be an angle at which sensor i observes the mth target, $f_{max,m}$ be the maximum Doppler frequency for target m, and T_p be the pulse duration. The normalized angle θ_{im} for target m and the normalized Doppler shift f_{im} when target m is moving relatively to sensor platform i are computed as [18]

$$\theta_{im} = \frac{d_i \sin \phi_{im}}{\lambda_i} \tag{3.6}$$

$$f_{im} = 4 f_{max,m} T_p \theta_{im} \tag{3.7}$$

We now assume that radar sensor i can detect M_i targets during the observation time. The received signal vector $\mathbf{z}_i(u,t)$ at sensor i is the superposition of signals reflected from M_i targets, interference, and noise.

$$\begin{aligned}\mathbf{z}_i(u,t) &= \sum_{m=1}^{M_i} \mathbf{e}(\theta_{im}, f_{im})\alpha_m(u)s_{mi}(t) + \mathbf{w}_i, \\ &= \mathbf{A}(\theta_i, f_i)\mathbf{s}_i(u,t) + \mathbf{w}_i, \quad i = 1, 2, ..., N.\end{aligned} \tag{3.8}$$

where

- $\mathbf{A}(\theta_i, f_i) = [\mathbf{e}(\theta_{i1}, f_{i1}), \mathbf{e}(\theta_{i2}, f_{i2}), ..., \mathbf{e}(\theta_{iM_i}, f_{iM_i})]$ is the $PK \times M_i$ target response matrix. $\mathbf{e}(\theta_{im}, f_{im})$ is a spatial-temporal steering vector that models the mth target return at angle θ_{im} and Doppler shift f_{im}.
- $\mathbf{s}_i(u,t) = [\alpha_1(u)s_{1i}(t), \alpha_2(u)s_{2i}(t), ..., \alpha_{M_i}(u)s_{M_i i}(t)]^T$ is the $M_i \times 1$ target signal vector with a random variable $\alpha_m(u)$ that models the radar cross section (RCS) of the target m and $s_{mi}(t)$ is the waveform reflected from target m.
- $\mathbf{w}_i = \mathbf{w}_{ci} + \mathbf{w}_{ji} + \mathbf{w}_{si} + \mathbf{n}_i$ represents the overall interference and noise: a clutter vector $\mathbf{w}_{ci}$, a jamming vector $\mathbf{w}_{ji}$, an interference vector between radar sensors $\mathbf{w}_{si}$, and thermal noise $\mathbf{n}_i$.

Received signals from radar sensors are forwarded to a central controller, e.g., clusterhead. Then, these received signal vectors $\mathbf{z}_i(u,t)$ are fused to make estimation operations. Since $\mathbf{z}_i(u,t)$ is a zero-mean Gaussian vector, the probability density function of $\mathbf{z}_i(u,t)$ can be presented as

$$f(\mathbf{z}_i(u,t)) = \frac{\exp\{-\frac{1}{2}\mathbf{z}_i^H[\mathbf{R}_{z,i}^{(\tau_i)}]^{-1}\mathbf{z}_i\}}{(2\pi)^{\frac{KP}{2}}|\mathbf{R}_{z,i}^{(\tau_i)}|^{\frac{1}{2}}}. \tag{3.9}$$

where $\mathbf{R}_{z,i}^{(\tau_i)}$ is the covariance matrix of $\mathbf{z}_i(u,t)$, τ_i is the rank of $\mathbf{R}_{z,i}$, and $|\cdot|$ denotes the determinant of the matrix.

3.4 Interference and Noise Model

As pointed out, at the ith radar sensor, the interference vector $\mathbf{w}_i$ is the sum of clutter $\mathbf{w}_{ci}$, jamming $\mathbf{w}_{ji}$, and interference between sensors $\mathbf{w}_{si}$. We apply the waveform design algorithm proposed in [31] to have waveforms at sensors be orthogonal. By doing so, interference between sensors can be negligible, i.e., $\mathbf{w}_{si} = \mathbf{0}$. Following are characteristics and models of clutter, jamming, and thermal noise at radar sensor i.

3.4.1 Clutter

Clutter generates undesired radar returns that may interfere with the desired signal. In RSN, the signal-to-clutter ratio (SCR) is often more important than the signal-to-noise ratio (SNR). The integrated clutter can be generally approximated as the sum of N_{ci} clutter patches. For clutter patch k, the space-time data vector is modeled as [18]

$$\begin{aligned} \mathbf{p}_{ki} &= \xi_{ki}\mathbf{b}_t(f_{ki}) \otimes \mathbf{a}_s(\theta_{ki}) \\ &= \xi_{ki}\mathbf{u}_{ki}, \quad k = 1, 2, ..., N_{ci}. \end{aligned} \tag{3.10}$$

where ξ_{ki} is a complex random variable that accounts for the amplitude and phase of clutter patch k. $\mathbf{u}_{ki} = \mathbf{b}_t(f_{ki}) \otimes \mathbf{a}_s(\theta_{ki})$ where $\mathbf{b}_t(f_{ki})$ and $\mathbf{a}_s(\theta_{ki})$ are temporal vector and spatial vector of clutter patch k, respectively. f_{ki} and θ_{ki} are the normalized Doppler shift and angle of arrival of the kth clutter patch, respectively. Total clutter vector $\mathbf{w}_{ci}$ equals to

$$\begin{aligned} \mathbf{w}_{ci} &= \sum_{k=1}^{N_{ci}} \xi_{ki}\mathbf{b}_t(f_{ki}) \otimes \mathbf{a}_s(\theta_{ki}) \\ &= \sum_{k=1}^{N_{ci}} \xi_{ki}\mathbf{u}_{ki}. \end{aligned} \tag{3.11}$$

The $KP \times KP$ covariance matrix of the clutter $\mathbf{R}_{ci}$ at the ith radar is given by

$$\begin{aligned} \mathbf{R}_{ci} &= E\{\mathbf{w}_{ci}\mathbf{w}_{ci}^H\} \\ &= \sum_{k=1}^{N_{ci}}\sum_{j=1}^{N_{ci}} E\{\xi_i\xi_j^H\}\mathbf{u}_{ki}\mathbf{u}_{ji}^H, \\ &= \sigma_{ci}^2\mathbf{M}_{ci}. \end{aligned} \tag{3.12}$$

where H denotes the Hermitian operation, $E\{\cdot\}$ denotes the expectation, and $\mathbf{M}_{ci}$ is the normalized covariance matrix, i.e., all diagonal entries of $\mathbf{M}_{ci}$ are ones.

3.4.2 Jamming

Jamming signals are generated by hostile interfering signal sources that seek to degrade the performance of radar sensors by mechanisms such as degrading signal-to-interference-plus-noise ratio (SINR) by increasing the noise level, or generating false detections to overwhelm RSN with false targets. A model for N_{ji} jamming signals is commonly presented as [45]

$$\mathbf{w}_{ji} = \sum_{l=1}^{N_{ji}} \beta_l \otimes a_{ji}(\theta_l), \quad i = 1, 2, ..., N. \tag{3.13}$$

where β_l contains voltage samples of the lth jamming waveform and $a_{ji}(\theta_l)$ is the jamming signal waveform at an angle θ_l. The different jamming waveforms are uncorrelated with each other.

3.4.3 Thermal Noise

Among noise existing in RSN, thermal noise due to ohmic losses at the radar receiver is normally dominant. We model the thermal noise vector $\mathbf{n}_i$ at radar sensor i as a complex white Gaussian vector with zero-mean and covariance σ_{ni}^2. The covariance matrix of noise $\mathbf{R}_{ni} = \sigma_{ni}^2\mathbf{I}$ where $\mathbf{I}$ is the $KP \times KP$ identity matrix.

In RSN, detection performance is largely affected by clutters. So we will consider the disturbance at the ith radar as a sum of thermal noise and clutter. The disturbance covariance matrix $\mathbf{R}_{wi}$ is given by

$$\begin{aligned} \mathbf{R}_{wi} &= E\{\mathbf{w}_i\mathbf{w}_i^H\} \\ &= \mathbf{R}_{ni} + \varepsilon_{ci}(h)\mathbf{R}_{ci}. \end{aligned} \tag{3.14}$$

where $\mathbf{R}_{ni}$ and $\mathbf{R}_{ci}$ are the covariance matrices of noise and clutter, respectively. $\varepsilon_{ci}(h)$ is a random variable used to model the clutter power of the hth range cell. $\varepsilon_{ci}(h)$ often

follows Weibull distribution for ground clutter or gamma distribution for sea and/or weather clutter [37][46]. In homogeneous environments, the average clutter power does not depend on h, i.e., $\varepsilon_{ci}(h)$ is constant. Therefore, the disturbance covariance matrix is rewritten as

$$\begin{aligned} \mathbf{R}_{wi} &= \sigma_{wi}^2 \mathbf{M}_{wi} \\ &= \sigma_{ni}^2 \mathbf{I} + \varepsilon_c \sigma_{ci}^2 \mathbf{M}_{ci}. \end{aligned} \tag{3.15}$$

where σ_{wi}^2 is the total disturbance power and $\mathbf{M}_{wi}$ is the normalized disturbance covariance matrix.

$$\mathbf{M}_{wi} = \frac{1}{CNR_i + 1}\mathbf{I} + \frac{CNR_i}{CNR_i + 1}\mathbf{M}_{ci}. \tag{3.16}$$

with $CNR_i = \frac{\varepsilon_c \sigma_{ci}^2}{\sigma_{ni}^2}$ is the clutter-to-noise power ratio. Then, total interference and noise can be modeled as a complex zero-mean white Gaussian vector with the covariance matrix $\sigma_{wi}^2 \mathbf{M}_{wi}$, i.e., $\mathbf{w}_i \sim \mathcal{CN}(0, \sigma_{wi}^2 \mathbf{M}_{wi})$.

3.5 Maximum Likelihood Multi-Target Detection (ML-MTD) Algorithm

In this section, we develop an algorithm to detect the number of targets in the sensing region. We assume that signals backscattered from targets and interference are uncorrelated. From the signal model in (3.8), the covariance matrix of received signal $\mathbf{z}_i(u,t)$ at radar sensor i is given by

$$\begin{aligned} \mathbf{R}_{z,i}^{(\tau_i)} &= E\{\mathbf{z}_i(u,t)\mathbf{z}_i^H(u,t)\}, \\ &= \mathbf{A}(\theta_i, f_i)\mathbf{R}_{s,i}\mathbf{A}^H(\theta_i, f_i) + \sigma_{wi}^2 \mathbf{M}_{wi}, \\ &= \mathbf{\Phi}_i^{(\tau_i)} + \sigma_{wi}^2 \mathbf{M}_{wi}. \end{aligned} \tag{3.17}$$

where $\mathbf{R}_{s,i}$ is a $M_i \times M_i$ positive definite matrix which represents the covariance matrix of the signal $\mathbf{s}_i(u,t)$, σ_{wi}^2 is the disturbance power, and $\mathbf{M}_{wi}$ is the normalized disturbance covariance matrix at radar sensor i. Matrices $\mathbf{R}_{s,i}$ and $\mathbf{\Phi}_i^{(\tau_i)}$ are defined:

$$\mathbf{R}_{s,i} = E\{\mathbf{s}_i(u,t)\mathbf{s}_i^H(u,t)\} \tag{3.18}$$

$$\mathbf{\Phi}_i^{(\tau_i)} = \mathbf{A}(\theta_i, f_i)\mathbf{R}_{s,i}\mathbf{A}^H(\theta_i, f_i) \tag{3.19}$$

The random variables $\alpha_m(u)$ $(i = 1, 2, ..., M_i)$ in $\mathbf{s}_i(u,t)$ model the RCS of the mth target. In [29], Swerling proposed five target models called Swerling models where Swerling V model is for non-fluctuating targets and Swerling I-IV models are for fluctuating targets. In this work, we focus our studies on the Swerling II target models. We know that magnitude of the RCS $|\alpha(u)|$ for Swerling II targets fluctuates independently from pulse to pulse according to a chi-square probability density function with two degree of freedom, i.e., a Rayleigh probability density function. Therefore, the RCS of target m can be modeled as a Gaussian random variable. That is,

$$\alpha_m(u) = \alpha_{Im}(u) + j\alpha_{Qm}(u). \tag{3.20}$$

where $\alpha_{Im}(u)$ and $\alpha_{Qm}(u)$ follow Gaussian distribution with zero mean and variance $\rho_m^2/2$ for each branch I, Q.

From (3.17), it follows that the rank of matrix $\mathbf{R}_{z,i}^{(\tau_i)}$ is τ_i, which is equal to the number of targets M_i present in the surveillance region, and the smallest $(KP - \tau_i)$ of its eigenvalues are zero, i.e., the received signal contains interference and noise only. Sorting the eigenvalues of $\mathbf{R}_{z,i}^{(\tau_i)}$ in a decreasing order, we obtain

$$\lambda_1 \geq \lambda_2 \geq ... \geq \lambda_{\tau_i}. \tag{3.21}$$

$$\lambda_{\tau_i+1} = \lambda_{\tau_i+2} = ... = \lambda_{KP} = \sigma_{wi}^2. \tag{3.22}$$

Assume that measurements $\mathbf{z}_i(u,t)$, at the clusterhead, are statistically independent complex Gaussian random vectors with zero mean. The joint probability density function of these random vectors has the form:

$$\begin{aligned} f(\mathbf{z}(u,t)) &= \prod_{i=1}^{N} f(\mathbf{z}_i(u,t)), \\ &= \prod_{i=1}^{N} \frac{\exp\{-\frac{1}{2}\mathbf{z}_i^H[\mathbf{R}_{z,i}^{(\tau_i)}]^{-1}\mathbf{z}_i\}}{(2\pi)^{\frac{KP}{2}}|\mathbf{R}_{z,i}^{(\tau_i)}|^{\frac{1}{2}}}. \end{aligned} \tag{3.23}$$

Basically, we have to estimate $\hat{\tau}_i$ such that the joint probability density function $f(\mathbf{z}(u,t))$ is maximized. We now define a log-likelihood function $\Gamma(\tau)$ $\{\tau = [\tau_1, \tau_2, ..., \tau_N]\}$ in (3.24). Hence, our mission is to find $\hat{\tau}_i$ such that $\Gamma(\tau)$ is minimized.

$$\begin{aligned}\Gamma(\tau) &= -\ln f(\mathbf{z}(u,t)), \\ &= \frac{N \times KP}{2}\ln(2\pi) + \frac{1}{2}\sum_{i=1}^{N}\log|\mathbf{R}_{z,i}^{(\tau_i)}| + \\ &+ \frac{1}{2}\sum_{i=1}^{N}\mathbf{z}_i^H[\mathbf{R}_{z,i}^{(\tau_i)}]^{-1}\mathbf{z}_i. \end{aligned} \tag{3.24}$$

Omitting terms that are independent of τ_i, we find the log-likelihood function $\Gamma(\tau)$.

$$\Gamma(\tau) = \sum_{i=1}^{N}\log|\mathbf{R}_{z,i}^{(\tau_i)}| + \sum_{i=1}^{N}\mathbf{z}_i^H[\mathbf{R}_{z,i}^{(\tau_i)}]^{-1}\mathbf{z}_i. \tag{3.25}$$

From [8], [19], and [7], the utility function $\Lambda(\tau)$ takes the form:

$$\Lambda(\tau) = \Gamma(\tau) + P(N). \tag{3.26}$$

where $P(N) = \wp(N)[\tau_{avg}(2KP - \tau_{avg})]$ is a bias correction term or penalty function to make estimate unbiased. τ_{avg} is an average value of $\{\tau_i | i = 1, 2, ..., N\}$ and $\wp(N)$ is a penalty coefficient which is a constant function of N. For example, $\wp(N) = 1$ for the Akaike information criterion (AIC) and $\wp(N) = \frac{1}{2}\ln N$ for the minimum description length (MDL). $\Lambda(\tau)$ then can be rewritten as

$$\begin{aligned}\Lambda(\tau) &= \sum_{i=1}^{N}\log|\mathbf{R}_{z,i}^{(\tau_i)}| + \sum_{i=1}^{N}\mathbf{z}_i^H[\mathbf{R}_{z,i}^{(\tau_i)}]^{-1}\mathbf{z}_i + \\ &+ \wp(N)\{\tau_{avg}(2KP - \tau_{avg})\}. \end{aligned} \tag{3.27}$$

Our ML-MTD algorithm to detect the number of targets $\widehat{M}$ present in the sensing field now can be expressed as

$$\widehat{M} = \lceil \frac{1}{N}\sum_{i=1}^{N}\hat{\tau}_i \rceil. \tag{3.28}$$

where $\hat{\tau} = \{\hat{\tau}_1, \hat{\tau}_2, ..., \hat{\tau}_N\}$ is computed as

$$\{\hat{\tau}_1, \hat{\tau}_2, ..., \hat{\tau}_N\} = \arg\min_{\tau_1, \tau_2, ..., \tau_N} \Lambda(\tau). \tag{3.29}$$

In practice, sensors can observe the different numbers of targets, i.e., τ_is may not be equal, since targets might not be exposed to all sensors. However, for the sake of simplicity, we assume that all radar sensors can observe the same number of targets, i.e., $\tau_1 = \tau_2 = ... = \tau_N = \tau$ and energy backscattered from targets is similar at radar sensors. Furthermore, we assume that the environment is homogeneous, that is, the average clutter power is a constant. These assumptions imply that $\mathbf{R}_{z,1}^{(\tau)} = \mathbf{R}_{z,2}^{(\tau)} = \mathbf{R}_{z,N}^{(\tau)} = \mathbf{R}_{z}^{(\tau)}$. For those reasons, our ultimate purpose is to evaluate detection performance improvement achievable by exploiting the networking of multiple radar sensors. Under our assumptions, the utility function $\Lambda(\tau)$ can be simplified as

$$\Lambda(\tau) = N \log |\mathbf{R}_{z}^{(\tau)}| + N\mathbf{tr}([\mathbf{R}_{z}^{(\tau)}]^{-1}\mathbf{Y}) + \wp(N)\{\tau(2KP - \tau)\}. \tag{3.30}$$

where $\mathbf{tr}(\cdot)$ denotes the trace of a matrix and $\mathbf{Y}$ is the sample covariance matrix of $\mathbf{z}_1, \mathbf{z}_2, ..., \mathbf{z}_N$.

$$\mathbf{Y} = \frac{1}{N}\sum_{i=1}^{N} \mathbf{z}_i \mathbf{z}_i^T. \tag{3.31}$$

Based on (3.30) and (3.31), we can observe that the utility function $\Lambda(\tau)$ depends on the number of radar sensors N. Our ML-MTD algorithm is used to determine any non-negative integer τ to minimize the utility function $\Lambda(\tau)$ when the number of radars is changed. Achieved results are analyzed to evaluate the multi-target detection performance in Section 3.6.

3.6 Multi-Target Detection Performance Analysis

We denote the true number of targets appearing in the observation area and the number of targets we can estimate from received signals as M and $\widehat{M}$, respectively. The probability of miss detection P_{MD} and the root mean square error (RMSE) are used as metrics to evaluate detection performance of the RSN using our proposed algorithm. We define P_{MD} and RMSE as follows:

- P_{MD} is the probability that the estimated number of targets is smaller than the true number of targets. Suppose that ω_{md} is the number of estimations in which

the estimated number of targets is smaller than the true number of targets and ω_t is the total number of estimations. P_{MD} is given as

$$\begin{aligned} P_{MD} &= P(\widehat{M} < M) \\ &= \frac{\omega_{md}}{\omega_t}. \end{aligned} \tag{3.32}$$

- RMSE is used to determine the vibration of the estimated number of targets $\widehat{M}$ around the true number of targets M.

$$RMSE = \sqrt{\frac{1}{\omega_t}\sum_{g=1}^{\omega_t}(M - \widehat{M}_g)^2}. \tag{3.33}$$

To study the MTD performance, we setup parameters for the RSN and targets as follows.

1. Spacing d_i between elements of the K-element ULA at radar sensor i is chosen to be a half of the wavelength λ_i, i.e., $d_i = \frac{\lambda_i}{2}$.
2. The pulse duration (T_p) is 1 ms.
3. The number of elements (K) in ULA is 5.
4. The number of pulses (P) in a coherent pulse interval is 4.
5. To observe targets, we assume that θ_{im} is a random variable which follows a uniform distribution in an interval [-0.5, 0.5].
6. The maximum Doppler frequencies for targets are similar, e.g., f_{max} = 5000Hz. The normalized Doppler shift f_{im} only depends on the random variable θ_{im}.
7. Average Signal-to-Interference-plus-Noise Ratio (SINR) refers to average SINR of all radars in RSN. We examine detection performance of RSN with average SINR in an interval [5dB, 15dB].
8. The MDL criterion is used for the penalty function.
9. 10^5 estimations are performed, i.e., $\omega_t = 10^5$.

We first examine the case in which there are three targets in surveillance region, i.e., $M = 3$. Single radar system, 4-radar RSN, and 8-radar RSN are employed to detect these targets. At each average SINR, the estimated number of targets is compared to the

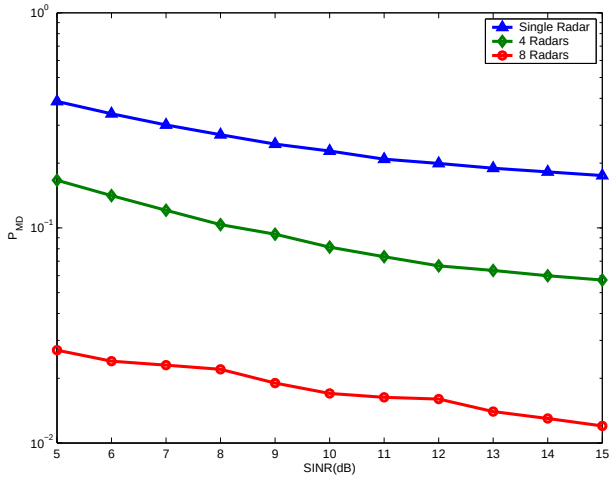

(a)

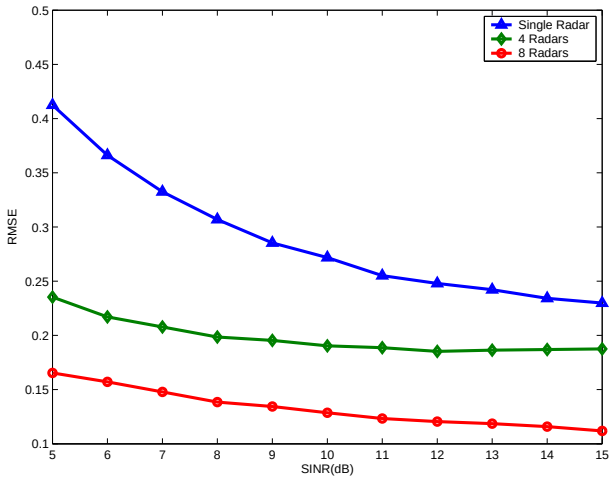

(b)

Figure 3.1: Miss-detection probability P_{MD} and RMSE, M=3

true number of targets to compute P_{MD} and RMSE which are drawn in Fig. 3.1 for this case. After that, we increase the number of targets into four, i.e., $M = 4$. Using the same RSN as the previous case, we can get P_{MD} and RMSE as plotted in Fig. 3.2. Based on achieved results in Fig. 3.1a and Fig. 3.2a, we can realize that miss-detection probability of 4-radar RSN and 8-radar RSN is much smaller than that of single radar system. This implies that detection performance of 4-radar RSN and 8-radar RSN is improved. For example, to achieve the same $P_{MD} = 10\%$ which is good enough according to Skolnik [14], the average SINR required for 4-radar RSN to detect three targets is about 9dB while the average SINR required for the single radar system is greater than 15dB. This means

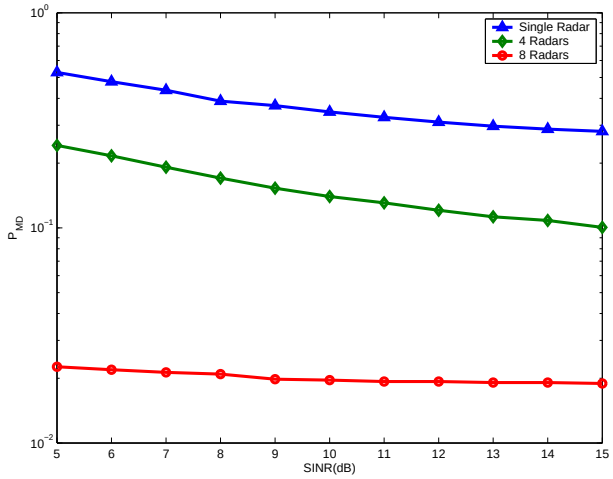

(a)

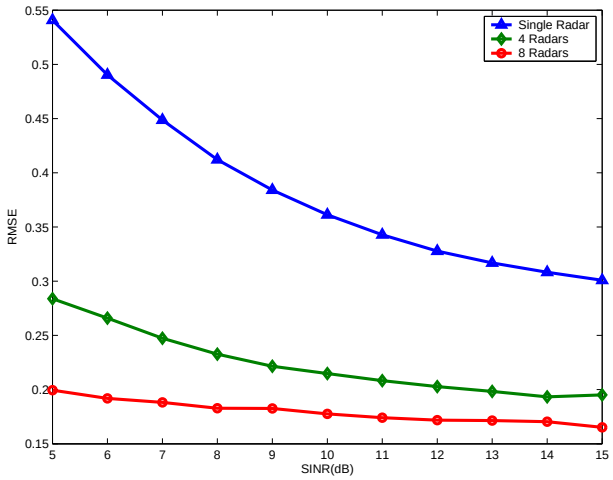

(b)

Figure 3.2: Miss-detection probability P_{MD} and RMSE, M=4

that detection performance gain of the 4-radar RSN is greater than 6dB. In both cases, moreover, the probability of miss-detection is vastly reduced when the 8-radar RSN is used.

Furthermore, we observe that the higher average SINR, the smaller probability of miss-detection. The reason is that, at high average SINR, radar sensors radiate signals at a high power level, so the coverage area of radar sensors is large. However, radiating signals at high power levels is costly. Thus tradeoff between cost and detection performance is necessary. We also observe that when we increase the number of targets, the detection performance is slightly reduced. For example, to achieve the same $P_{MD} = 10\%$,

the 4-radar RSN to detect four targets requires average SINR around 4dB higher than that to detect three targets. This means that we need increase the transmit power for radar sensors. If the number of sensor radars is however large, e.g. $N = 8$, the detection performance of the RSN does not change much.

Besides the miss-detection probability, RMSE is the other metric to examine the detection performance of the RSN. RMSE helps us evaluate the variability of the estimated number of targets around the true number of targets present in the sensing field. From Fig. 3.1b and Fig. 3.2b, we note that, to estimate three or four targets, RMSE of a single radar system is very high while RMSE of RSN is reduced tremendously. For example, at SINR = 9dB, compared to a single radar system, the 4-radar RSN can reduce RMSE by 31.52% for three target case and 42.32% for four target case. Moreover, we can see that RMSE is reduced when we increase the number of sensors and/or average SINR.

3.7 Conclusions

We investigate a multi-target detection problem in Radar Sensor Networks. Signal, interference, and noise models at radar sensors are presented and analyzed. We also propose a Maximum Likelihood Multi-Target Detection algorithm to estimate the possible number of targets in a surveillance area. RSN-clusterhead utilizes our algorithm to combine measurements from radar sensors and make decision. Achieved results show that detection performance of our RSN is much better than that of a single radar system in terms of the miss-detection probability and the root mean square error.

CHAPTER 4

OPPORTUNISTIC SPECTRUM ACCESS IN COGNITIVE SENSOR NETWORKS

4.1 Introduction

Recent measurements have shown that, with the traditional spectrum access approach, the radio spectrum assigned to primary (licensed) users is vastly underutilized while the demand for access to the limited radio spectrum has been growing dramatically. This view is supported by actual measurements conducted by the FCC's Spectrum Policy Task Force which has determined that, in some locations or at some times of a day, about 70 percent of the allocated spectrum may not be in use [40]. Measurements in [23] reveal that spectrum utilization is often heavy in unlicensed bands while low in TV bands or medium in some cellular bands. These observations on actual spectrum usage have challenged approaches to the radio spectrum management and fueled interests in the opportunistic spectrum access problem.

Opportunistic spectrum access (OSA) has been enabled by cognitive radios (CRs) which have capabilities to sense their surroundings and actively adapt their operation modes to maximize the quality of service for secondary users (SUs) while minimizing interference to primary users (PUs). Hence, CRs must carry out spectrum sensing to identify white spaces or spectrum holes which are bands of frequencies assigned to PUs, but, at a particular time and a specific geographic location, these bands are not being utilized by those users [41]. Some methods on spectrum sensing have been proposed in [39], [2], and [13]. Once spectrum holes are identified, CRs opportunistically utilize these holes for communications without causing harmful interference to PUs. Assume that a spectrum band is available for SUs. If only one SU, in a particular location and at a specific time, can sense this available spectrum, this SU can use this band right after

the PU finishes its communications session. In the case of multiple SUs trying to access the spectrum, however, SUs are supposed to compete with each other in a collaborative and fair manner to access the spectrum.

Amongst existing work on spectrum sharing, the work in [34] and [28] applied game-theoretic framework to find strategies for spectrum sharing. In [12], spectrum allocation using a graph coloring algorithm is proposed but mobility of the secondary users is not considered. Moreover, authors assumed that if two SUs within distance of each other use the same spectrum band, they fail to access spectrum. With this approach, some SUs will lose the rights to compete for using spectrum and monitoring SUs conflicting in using spectrum band is also a challenging issue. In [13], some other spectrum sharing methods were summarized.

In this chapter, we propose a Knowledge-based Spectrum Access Scheme to efficiently assign the available spectrum for SUs and guarantee that the SU using assigned band will not interfere with PUs. To achieve these objectives, our scheme is designed using FLS with three descriptors: spectrum utilization efficiency of the SU, its degree of mobility, and its average distance to PUs. To increase the reliability of our method, the linguistic knowledge of spectrum access based on these descriptors is obtained from a group of network experts. 27 fuzzy spectrum sharing rules are set up based on this linguistic knowledge. The output of the FLS provides the probability of assigning spectrum for each SU and the SU with the highest probability will access the available spectrum.

The rest of this chapter is organized as follows. In Section 4.2, we briefly introduce the fuzzy logic system. The knowledge-based spectrum access scheme is proposed in Section 4.3. In Section 4.4, we discuss the simulation results and conclusions are presented in Section 4.5.

4.2 Fuzzy Logic Systems

Fig. 4.1 shows the structure of a fuzzy logic system (FLS). When an input is applied to the FLS, the inference engine computes the output set corresponding to each rule. The

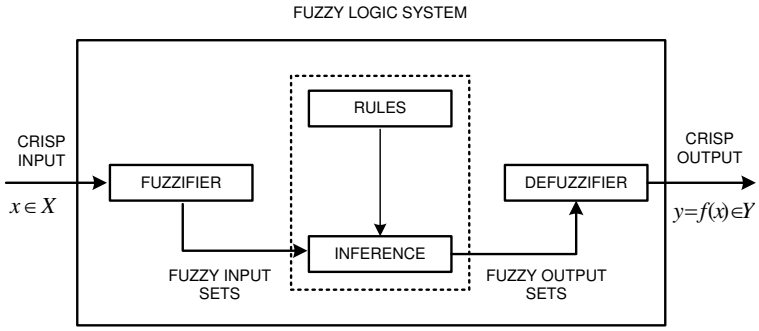

Figure 4.1: The structure of a Fuzzy Logic System

defuzzifier then computes a crisp output from these rule output sets. Consider a p-input 1-output FLS, using singleton fuzzification, center-of-sets defuzzification and IF-THEN rules of the form [16]

$$R^l\text{: IF } x_1 \text{ is } F_l^1 \text{ and } x_2 \text{ is } F_l^2 \text{ and ... and } x_p \text{ is } F_l^p,$$
$$\text{THEN y is } G^l$$

Assuming singleton fuzzification is used, when an input $\mathbf{x}' = \{x_1', x_2', ..., x_p'\}$ is applied, the degree of firing corresponding to the lth rule is computed as

$$\mu_{F_1^l}(x_1') \star \mu_{F_2^l}(x_2') \star ... \star \mu_{F_p^l}(x_p') = \mathcal{T}_{i=1}^p \mu_{F_i^l}(x_i') \tag{4.1}$$

where $\star$ and $\mathcal{T}$ both indicate the chosen t-norm. There are many kinds of defuzzifiers. In this work, we focus, for illustrative purposes, on the center-of-sets defuzzifier. It computes a crisp output for the FLS by first computing the centroid, c_{G^l}, of every consequent set G^l, and, then computing a weighted average of these centroids. The weight corresponding to the lth rule consequent centroid is the degree of firing associated with the lth rule, $\mathcal{T}_{i=1}^p \mu_{F_i^l}(x_i')$, so that

$$y_{cos}(\mathbf{x}') = \frac{\sum_{l=1}^M c_{G^l} \mathcal{T}_{i=1}^p \mu_{F_i^l}(x_i')}{\sum_{l=1}^M \mathcal{T}_{i=1}^p \mu_{F_i^l}(x_i')} \tag{4.2}$$

where M is the number of rules in the FLS.

4.3 Knowledge Processing and Knowledge-based Spectrum Access Scheme

4.3.1 Knowledge-based Spectrum Access Scheme Design

We design a Knowledge-based Spectrum Access Scheme using a fuzzy logic system to solve the opportunistic spectrum access problem in cognitive radio networks. Expert knowledge for selecting the best suitable SU to access the available band is collected based on the following three antecedents:

1. Antecedent 1: Spectrum utilization efficiency.
2. Antecedent 2: Degree of mobility.
3. Antecedent 3: Average distance to primary users.

Generally, the SU with the furthest average distance to PUs or the SU with maximum spectrum utilization efficiency can be chosen to access spectrum under the constraint that no harmful interference is created for PUs. In our approach, using the rule-based FLS, we combine the above descriptors to assign spectrum opportunistically. We observe that different users perceive different available spectrum and using spectrum efficiently is the main purpose of the OSA schemes. For that reason, spectrum utilization efficiency η_s is introduced in our design. η_s is defined as the ratio between the spectrum BW_s which SU desires to utilize and the available band BW_a, i.e.,

$$\eta_s = \frac{BW_s}{BW_a} \times 100\% \tag{4.3}$$

Mobility of SUs plays an important role in our design. When SU is moving at a velocity $v\ m/s$, it generates the Doppler shift f_D.

$$f_D = \frac{v}{c} f_c \tag{4.4}$$

where f_c is carrier frequency and c is the speed of light ($3 \times 10^8 m/s$). Mobility of SUs can reduce capability of detecting signal from PUs. If SU is not capable of detecting the primary signal, it will incorrectly determine that the spectrum is unused; thereby leading to potential interference to adjacent users, i.e., the signal transmitted by SU will interfere with the signal that PU is trying to decode. This situation is often referred as the *hidden node problem*.

Moreover, we also consider the average distance between SU and PUs. The location of PUs can be obtained via GPS (Global Positioning System) or other position location technologies. If the location of PUs is unknown, we can consider signal-to-noise ratio (SNR) as a proxy for distance [27]. Assume the PU at the distance d_i from SU i transmits signal at power P_{1i} and the power gain between PU and SU, $g(d_i)$, is a continuous, nonnegative, strictly decreasing function of d_i defined on the interval $[0, \infty]$.

$$\gamma_{si} = 10log(\frac{P_{1i}g(d_i)}{\sigma_1^2}) \tag{4.5}$$

where γ_{si} and σ_1^2 are the SNR and noise power measured at the SU i, respectively.

Linguistic variances to represent Antecedent 1 and Antecedent 2 are divided into three levels: *low, moderate,* and *high* while we use three levels: *near, moderate,* and *far* to represent Antecedent 3. Five levels, i.e., *very low, low, medium, high*, and *very high* are used for the consequence. We use trapezoidal membership functions (MFs) to represent *near, low, far, high, very low,* and *very high*; and triangle MFs to represent *moderate, low, medium*, and *high*. Designed MFs are shown in Fig. 4.2. Since we have 3 antecedents and 3 fuzzy subsets, we need to set up 3^3 rules for our FLS. Then, we design questions used in our survey according to rules as follows:

IF *spectrum utilization efficiency of the secondary user is moderate, its degree of mobility is low, and its average distance to primary users is far*, THEN *the probability that this user is selected to access the spectrum is* _____.

4.3.2 Knowledge Processing for Spectrum Access Scheme

As pointed out in [17], "words mean different things to different people", and in [21], "the decision makers may have the same preferences to a particular alternative, e.g., highly preferred but with different degrees;" so, we created one survey for the network experts. These experts were requested to choose a consequent, using one of the five linguistic variables. Different experts gave different answers to the questions in the survey. Table 4.1 summarizes the questions used in our survey. As an example, we give an expert's

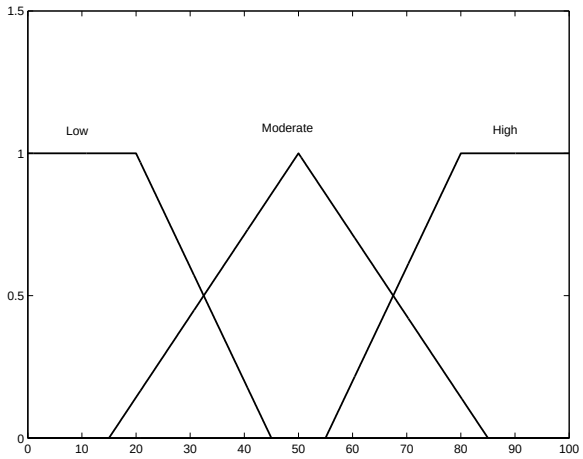

(a)

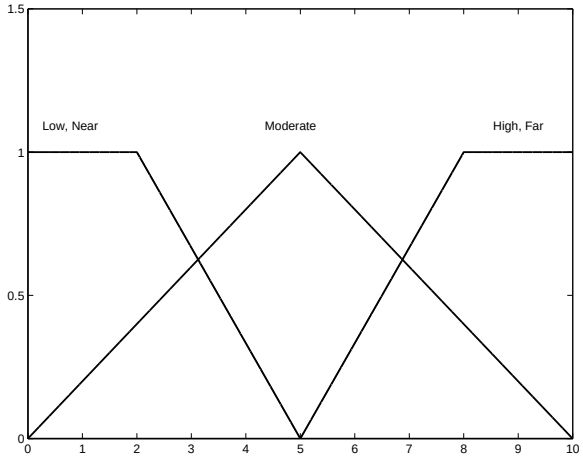

(b)

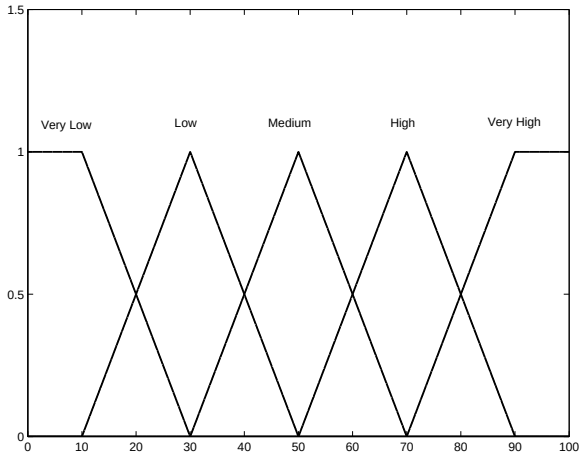

(c)

Figure 4.2: Membership functions (MFs) representing linguistic labels for: (a) Antecedent 1, (b) Antecedent 2 and 3, and (c) Consequence.

Table 4.1: Questions for opportunistic spectrum access problem

Rule #	Antecedent 1	Antecedent 2	Antecedent 3	Consequence
1	low	low	near	*very low*
2	low	low	moderate	*low*
3	low	low	far	*low*
4	low	moderate	near	*very low*
5	low	moderate	moderate	*low*
6	low	moderate	far	*medium*
7	low	high	near	*very low*
8	low	high	moderate	*low*
9	low	high	far	*medium*
10	moderate	low	near	*very low*
11	moderate	low	moderate	*medium*
12	moderate	low	far	*high*
13	moderate	moderate	near	*very low*
14	moderate	moderate	moderate	*medium*
15	moderate	moderate	far	*high*
16	moderate	high	near	*very low*
17	moderate	high	moderate	*low*
18	moderate	high	far	*high*
19	high	low	near	*low*
20	high	low	moderate	*high*
21	high	low	far	*very high*
22	high	moderate	near	*low*
23	high	moderate	moderate	*high*
24	high	moderate	far	*very high*
25	high	high	near	*very low*
26	high	high	moderate	*high*
27	high	high	far	*high*

answer in the table. Since we chose a single consequent for each rule to form a rule base, we averaged the centroids of all the responses for each rule and used average values in place of the rule consequent centroid. Doing this leads to rules with the following form:

R^l: IF *spectrum utilization efficiency of the secondary user* (x_1) is F_l^1, and *its degree of mobility* (x_2) is F_l^2, and *its average distance to primary users* (x_3) is F_l^3, THEN the probability (y) that this secondary user is chosen to access the available spectrum is c_{avg}^l ($l = 1, 2, ..., 27$).

$$c_{avg}^l = \frac{\sum_{i=1}^{5} w_i^l c^i}{\sum_{i=1}^{5} w_i^l} \tag{4.6}$$

Table 4.2: Values of c_{avg} corresponding to each rule

Rule #	c_{avg}	Rule #	c_{avg}
1	17.222	15	63.33
2	23.611	16	17.22
3	43.333	17	30.278
4	23.611	18	56.667
5	30	19	50
6	43.333	20	70
7	10.833	21	89.167
8	23.611	22	36.667
9	36.667	23	63.333
10	30.278	24	82.778
11	56.667	25	30.287
12	76.389	26	56.667
13	23.889	27	63.333
14	43.333		

Table 4.3: Three descriptors and spectrum access probability for four SUs

Parameters	SU1	SU2	SU3	SU4
Mobility degree	2.4966	3.0715	6.5382	0.9135
Distance to PU	8.4852	3.0036	10	1.6437
Probability	82.2944	54.5189	45.3072	53.1432
Spectrum usage efficiency	88.7104%	97.9340%	24.2160%	92.4424%

in which w_i^l is the number of experts choosing linguistic label i for the consequence of rule l and c^i is the centroid of the ith consequence set ($i = 1, 2, ..., 5$). Table 4.2 provides c_{avg} for each rule from the completed survey. For every input (x_1, x_2, x_3), the output $y(x_1, x_2, x_3)$ of the designed FLS is computed as

$$y(x_1, x_2, x_3) = \frac{\sum_{l=1}^{27} \mu_{F_1^l}(x_1)\mu_{F_2^l}(x_2)\mu_{F_3^l}(x_3)c_{avg}^l}{\sum_{l=1}^{27} \mu_{F_1^l}(x_1)\mu_{F_2^l}(x_2)\mu_{F_3^l}(x_3)} \tag{4.7}$$

We recognize that (4.7) can be represented in a 4-D surface. Since it is impossible to plot it visually, we fix one of three variables. More specifically, we fixed the average distance to the primary users x_3 and kept x_1 and x_2 as random variables. Two cases, i.e., $x_3 = 1$ and $x_3 = 9$, were considered. Fig. 4.3 represents a decision surface for the cognitive users in these cases. The concept of decision surface, which is central in fuzzy logic systems, describes the dynamics of the controller and is generally a time-varying

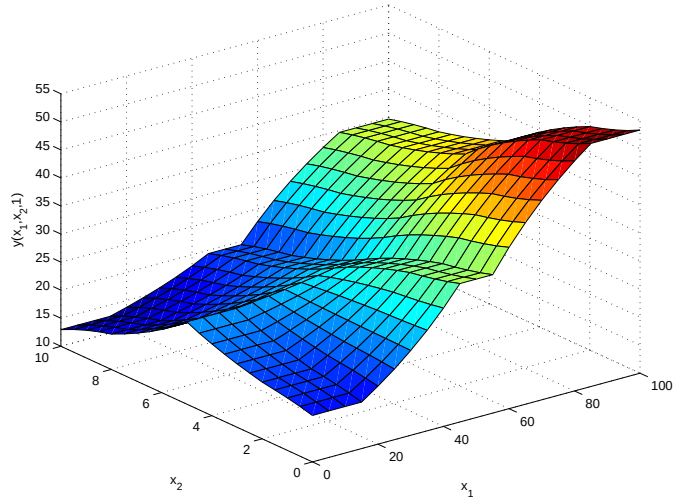

(a)

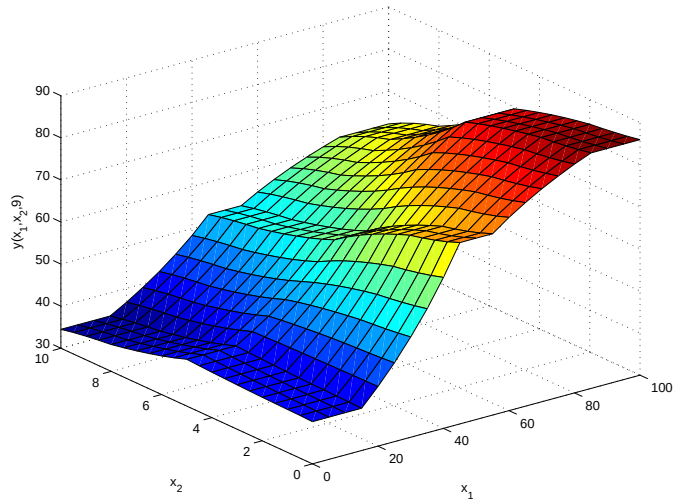

(b)

Figure 4.3: Decision surface for cognitive users with a fixed average distance to primary users: (a) $x_3 = 1$, (b) $x_3 = 9$.

nonlinear surface. From Fig. 4.3, we see clearly that, at the same spectrum utilization efficiency and mobility degree, SUs further from PUs have higher chance to access the spectrum.

4.4 Simulation Results and Discussion

To validate our approach, we randomly generated 20 SUs over an area of 100×100 meters. Assume that an PU was placed randomly in this area. Three descriptors were

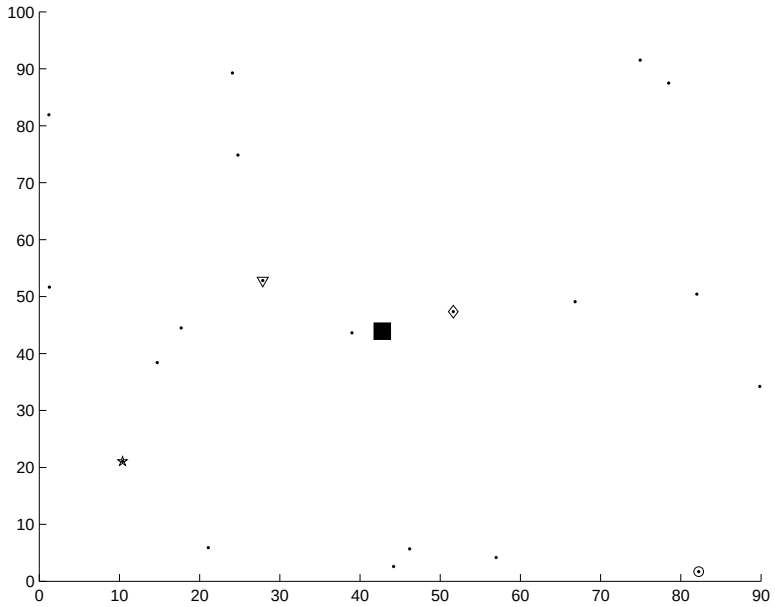

Figure 4.4: An OSA scenario example: SU1, SU2, SU3, and SU4 are denoted using $\star$, $\bigtriangledown$, $\circ$, and $\Diamond$, respectively. The primary user is denoted using $\square$.

randomly generated for each SU. More specifically, the spectrum utilization efficiency of each secondary user was a random value in the interval $[0, 100]$ and its mobility degree in $[0, 10]$. Distances to the PU were normalized to $[0, 10]$.

$$d_i = \sqrt{(x_i - x_p)^2 + (y_i - y_p)^2} \tag{4.8}$$

where (x_p, y_p) and (x_i, y_i) represent the coordinate of the PU and the ith SU ($i = 1, 2, ..., 20$).

The values of descriptors corresponding to each SU were passed through the FLS. The output of the FLS, i.e., the probability that a SU was selected to access the available spectrum, was computed in (4.7). Then, the SU with the highest probability would be chosen to access the spectrum.

At a particular time, values of three descriptors and probability for four SUs, i.e., the SU chosen to access the available spectrum (SU1), the SU with the highest spectrum utilization efficiency (SU2), the SU having the furthest distance to the primary user (SU3), and the SU with the lowest mobility degree (SU4) are listed in Table 4.3. Position of these users is shown in Fig. 4.4 while spectrum usage efficiency of SUs is drawn in

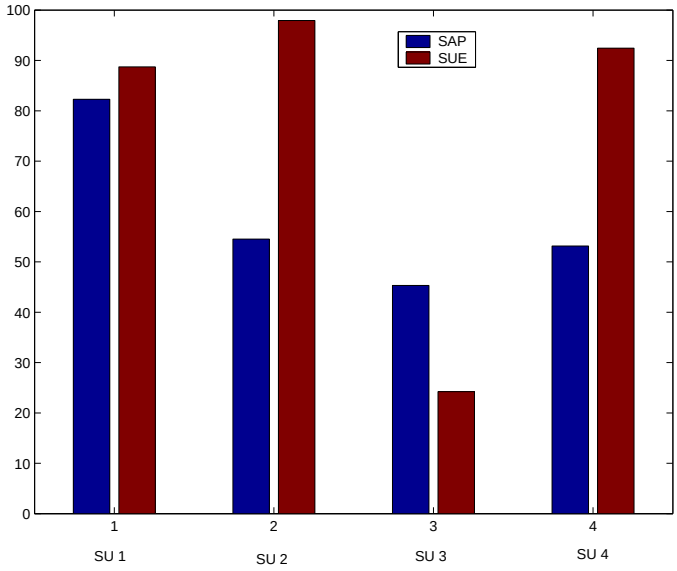

Figure 4.5: Spectrum Utilization Efficiency (SUE) and Spectrum Access Probability (SAP) for SU1, SU2, SU3, SU4

Fig. 4.5. From the graph, we note that SU2 has the highest spectrum utilization efficiency with 97.93%, SU4 with 92.4424% while SU1 only achieves 88.7104%. Although SU3 is the SU with the furthest distance, it has the lowest spectrum utilization efficiency and highest mobility degree.

In wireless networks, the radio link quality is usually limited by interference rather than noise. Therefore, the outage probability due to co-band is of primary concern and can be determined by the Signal-to-Interference Ratio (SIR). SIR measured at the receiver j associated with transmitter i can be expressed as:

$$SIR_{ij} = \frac{P_i G_{ji}}{\sum_{k=1,k\neq i}^{N} P_k G_{jk} I(k,j) + \delta^2} \tag{4.9}$$

where P_i is the transmission power at transmitter i, G_{ji} is the link gain between transmitter i and receiver j. δ^2 denotes the received noise and it is assumed to be the same for all receiver nodes. $I(i;j)$ is the interference function characterizing the interference created by node i to node j.

$$I(i;j) = \begin{cases} 1 & \text{if transmitters } i \text{ and } j \text{ are transmitting over the same band} \\ 0 & \text{otherwise} \end{cases}$$

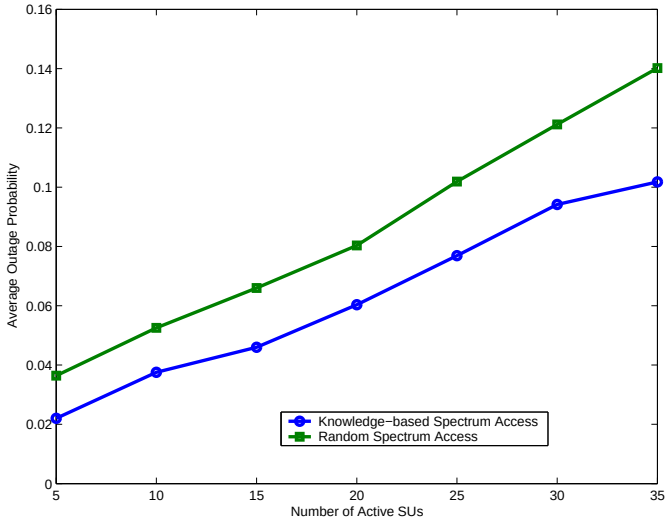

Figure 4.6: Outage Probability vs. Number of Secondary Users

We assume the QoS requested is guaranteed when the SIR_{ij} exceeds a given threshold SIR^{th}. The outage probability P_{out} of the jth receiver/ith transmitter pair is given by

$$\begin{aligned} P_{out} &= P_r(SIR_{ij} \leq SIR^{th}) \\ &= P_r(P_i G_{ji} \leq SIR^{th}(\sum_{k=1,k\neq i}^{N} P_k G_{jk} I(k,j) + \delta^2)) \end{aligned} \tag{4.10}$$

Fig. 4.6 show the relation between the outage probability and the number of active SUs. From the graph, we can recognize that our proposed approach successfully reduced the outage probability by about 20% which implies a higher probability that the received signal level will exceed SNR^{th}. Hence, the quality of communications of adjacent users can be guaranteed.

Until now, someone may have two more questions: (1) who will decide the spectrum access rights for SUs? (2) if there are N users competing for M spectrum bands ($N >> M$), how can we control the spectrum access? Since we use the centralized spectrum sharing architecture, a centralized entity such as base stations in cognitive wireless networks or clusterheads in sensor networks collects information about three descriptors and available spectrum bands from SUs through a common control channel and dynamically builds a spectrum map. Then, it uses our proposed knowledge-based spectrum

access scheme to control the spectrum assignment and access procedures in order to prevent multiple users from colliding in overlapping spectrum portions. In case, N users competing for M spectrum bands, the centralized processor also takes advantage of our scheme for each band to allow the best secondary user to access each spectrum.

4.5 Conclusions

We propose a knowledge-based spectrum access scheme which is built on the rule-based fuzzy logic system to control opportunistic spectrum access for SUs in cognitive radio networks. The SU is selected based on combination of spectrum utilization efficiency of SU, its degree of mobility, and its average distance to PUs. The linguistic knowledge of spectrum access is based on experiences from a group of network experts instead of only a single one, so that an acceptable decision could be obtained. Moreover, we can modify the membership functions in our design in accordance to requirements of the primary network and the spectrum usage policy. To validate our approach, an OSA scenario is simulated and analyzed. We also show that our scheme could decrease the outage probability compared to the random access method. Then, our scheme is promising to be implemented practically in future cognitive radio networks.

CHAPTER 5

CONCLUSIONS AND FUTURE DIRECTIONS

5.1 Conclusions

In this thesis, we have discussed the target detection problem in Radar Sensor Networks (RSN) and opportunistic spectrum access in Cognitive Sensor Networks (CSN). Two main detection problems in RSN have been addressed:

- Improving the target detection performance using our proposed diversity, which is based on the combination of STAP technique and waveform design, is discussed and analyzed. Studies show that the detection performance in term of miss-detection probability and false alarm probability of the RSN using our diversity scheme is superior to that of the single radar system using STAP only.
- Estimating the number of targets present in the surveillance field is discussed. At the clusterhead, an algorithm to detect the number of targets is also developed based on measurement data at radar sensors. Simulation results confirm that the multi-target detection performance of RSN in terms of the miss-detection probability and the root mean square error is much better than that of the single radar system.

We also studied the spectrum access problem in cognitive sensor networks. A spectrum access scheme using the fuzzy logic system is proposed. We show that our spectrum access scheme performs much better than a random spectrum access scheme.

5.2 Future Directions

Besides our studies presented in this thesis, we can extend our research in several directions as follows:

5.2.1 Detection in Radar Sensor Networks

- The performance of RSN is affected by other factors such as crab angle, mutual coupling, and beam mismatch between target and steering vector. Therefore, target detection performance can be examined when these factors exist.
- This thesis studies detection problems in the homogeneous environment. So detection problem when interference environment is heterogeneous can be investigated.
- Using the diversity scheme proposed in the chapter 2 to solve advanced problems in radar sensor networks such as target search and target recognition is also worth looking into.
- Target models as small moving point-like targets in our detection problems are considered in this thesis. Thus dynamic and state space-based models might be further studied.
- Naturally, multiple target model types can appear during observation, so multi-target detection problem when multiple target models coexist in the sensing region is worth looking into.
- Our proposal to estimate the number of targets in a surveillance region is a primary state for important tasks such as target recognition, classification, tracking, etc. A joint algorithm to combine multi-target detection and one of above tasks can be investigated.

5.2.2 Opportunistic Spectrum Access in Cognitive Sensor Networks

In Multi-Hop Cognitive Sensor Networks, cognitive users experience spectrum heterogeneity, i.e., their spectrum availability fluctuates over time and location. We know that existing work on general routing problem for wireless networks has been well investigated. However, they do not consider spectrum fluctuation in their routing algorithms. Therefore, a joint spectrum opportunity discovery and routing scheme can be examined. To evaluate the performance of this scheme, throughput and latency can be used as evaluation metrics.

REFERENCES

[1] B. R. Mahafza, *Radar Systems Analysis and Design*, Chapman & Hall, 2005.

[2] B. Wild and K. Ramchandran, "Detecting primary receivers for cognitive radio applications," *IEEE Proc. on DySPAN 2005, Nov. 2005.*

[3] C. E. Baum *et al.*, "The singularity expansion method and its application to target identification," *Proc. of the IEEE,* vol 79, no. 10, Oct. 1991.

[4] C. J. Baker, A. L. Hume, "Netted Radar Sensing," *IEEE A&E Systems Magazine,* Feb. 2002.

[5] C. R. Lin and M. Gerla, "Adaptive Clustering for Mobile Wireless Networks," *IEEE journal on selected areas in communications,* vol. 15, no. 7, Sep. 1997.

[6] F. Gini *et al.*, "Multiple target detection and estimation by exploiting the amplitude modulation induced by antenna scanning. Part II: Detection ," IEEE ICASSP, pp 533-536, 2003.

[7] G. Schwartz, "Estimating the dimension of a model," *Annals of Statistics,* vol. 6, pp. 497-511, 1978.

[8] H. Akaike, "A new look at the statistical model identification," *IEEE Transactions on Automatic Control,* vol 19, pp 716-723, Dec. 1974.

[9] Hung D. Ly and Q. Liang, "Spatial-Temporal-Frequency Diversity in Radar Sensor Networks," *IEEE Military Communications Conference,* Oct. 2006, Washington DC.

[10] Hung D. Ly and Q. Liang, "Collaborative Multi-Target Detection in Radar Sensor Networks," submitted to *IEEE Military Communications Conference,* Oct. 2007, Orlando FL.

[11] H. Wang and L. Cai, "A localized adaptive MTD processor," *IEEE Transaction on Aerospace and Electronic Systems,* vol 27, no.3, pp. 532-539, 1991.

[12] H. Zheng and C. Peng, "Collabraton and fairness in opportunistic spectrum access," *IEEE International Conf. on Communications, 2005.*

[13] I. F. Akyildiz, *et al*, "NeXt generation/dynamic spectrum access/cognitive radio wireless networks: A survey," *Computer Networks Journal (Elsevier),* vol. 50, pp. 2127-2159, September 2006.

[14] I. Skolnik, *Introduction to Radar Systems*, 3rd ed, McGraw Hill, 2001.

[15] J. Goldstein, L. Scharf, and I. Reed, "A multistage representation of the Wiener filter based on orthogonal projections," *IEEE Transaction on Information Theory,* vol. 44, no. 7, pp. 2943-2959, 1998.

[16] J. M. Mendel, *Uncertanty Rule-based Fuzzy Logic Systems*, Prentice Hall, Upper Saddle River, NJ, 2001.

[17] J. M. Mendel, "Computing with words when words can mean different things to different people," *Int'l ICSC Congress on Computational Intelligence: Methods and Applications,* NY, Jun. 1999.

[18] J. R. Guerci, *Space-Time Adaptive Processing for Radar*, Artech House, 2003.

[19] J. Rissanen, "A universal prior for intergers and estimation by minimum description length," *Annals of Statistics,* vol. 11, no. 2, pp. 431-466, 1983.

[20] J. Ward, "Space-Time Adaptive Processing for Airborne Radar," *Lincoln Laboratory Technical Report 1015,* Dec. 1994.

[21] Marimin *et al.*, "Linguistic labels for expressing fuzzy preference relations in fuzzy group decisio making," *IEEE Trans. on Systems, Man, and Cybernetics - Part B: Cybernetics*, vol. 28, no. 2, Apr. 1998.

[22] M. A. Richards, *Fundamentals of Radar Signal Processing*, McGraw-Hill Companies, New York 2005.

[23] M. McHenry, "Report on spectrum occupancy measurements," shared spectrum company.

[24] M. R. Bell, "Information theory and radar waveform design," *IEEE Transaction on Information Theory,* vol. 39, no. 5, pp. 1578-1597, Sept. 1993.

[25] M. Wax and T. Kailath, "Detection of signals by information theoretic criteria," *IEEE Transactions on Acoustics, Speech, and Signal Processing,* vol 33, no.2, pp 387-392, April 1985.

[26] M. Kaveh *et al.*, "On the theoretical performance of a class of estimators of the number of narrow-band sources," *IEEE Trans. on Acoustics, speech, and signal processing,* no.9, Sept. 1987.

[27] N. Hoven and A. Sahai, "Power scaling for cognitive radio," *International Conference on Wireless Networks, Communications and Mobile Computing*, vol. 1, Jun. 2005, pp. 250-255.

[28] N. Nie and C. Comaniciu, "Adaptive channel allocation spectrum atiquette for cognitive radio networks," *IEEE Pro. on DySPAN 2005, Nov. 2005.*

[29] P. Swerling, "Probability of Detection for Fluctuating Targets," *IRE Transactions on Information Theory,* vol IT-6, pp. 269-308, April 1960.

[30] Q. Liang, "Radar Sensor Networks: Algorithms forWaveform Design and Diversity with Application to ATR with Delay-Doppler Uncertainty," *EURASIP Journal on Wireless Communications and Networking,* Volume 2007, Article ID 89103.

[31] Q. Liang, "Waveform design and diversity in radar sensor networks: Theoretical analysis and application to Automatic Target Recognition," *Workshop on Wireless Ad Hoc and Sensor Networks,* June 2006, New York.

[32] Q. Liang, "Clusterhead election in mobile ad hoc networks," *IEEE Proc.on Personal, Indoor and Mobile Radio Communications*, vol. 2, Sept. 2003, pp. 1623 - 1628.

[33] Q. T. Zhang *et al.*, "Statistical Analysis of the performance of Information Theoretic Criteria in the detection of the number of signals in array processing," *IEEE Trans. on Acoustics, speech, and signal processing,* pp 1557-1565, vol. 37, no.10, Oct. 1989.

[34] R. Etkin, A. Parekh and D. Tse, "Spectrum Sharing for Unlicensed Bands," IEEE Proc. on DySPAN 2005, Nov. 2005.

[35] R. Fitzgerald, "Effects of range-doppler coupling on chirp radar tracking acuracy," *IEEE Trans on Aerospace and Eletronic Systems,* vol. 10, pp. 528-532, July 1974.

[36] R. Klemm, "Introduction to Space-Time Adaptive Processing," *Electronics & Communication Engineering Journal,* Feb. 1999.

[37] R. Nitzberg, "An effect of range-heterogeneous clutter on adaptive doppler filters," *IEEE Transaction on Aerospace and Electronic Systems, vol 26, no.3, pp 475-480, May 1990.*

[38] R. S. Adve *et al.*, "Practical Joint Domain Localized Adaptive Processing in Homogeneous and Non-homogeneous Environments: Part I - Homogeneous Environments," *IEE Part F: Proceedings on Radar, Sonar and Navigation,* Oct. 1999.

[39] R. Tandra and A. Sahai, "Fundamental limits on detection in low SNR under noise uncertainty," *International Conference on Wireless Networks, Communications and Mobile Computing*, vol. 1, Jun. 2005, pp.464-469.

[40] Spectrum Policy Task Force report, Technical report 02-135, Federal communications commission, Nov. 2002.

[41] S. Haykin, "Cognitive radio: Brain-empowered wireless communication," *IEEE Journal on Selected Areas in Communications,* vol. 23, no. 5, Feb 2005, pp. 201-220.

[42] S. Kadambe, "Feature discovery and sensor discrimination in a network of distributed radar sensors for target tracking," *HRL Laboratories, LLC, 2001.*

[43] S. M. Kay, *Fundamentals of Statistical Signal Processing: Detection Theory*, Prentice Hall, 1993.

[44] T. K. Sarkar and N. Sangruji, "An adaptive nulling system for a narrow-band signal with a look-direction constraint utilizing the conjugate gradient method," *IEEE Transaction on Antennas and Propagation*, vol. 37, no. 7, pp. 940-944, July 1989.

[45] W. L. Melvin, "A STAP Overview," *IEEE A&E Systems Magazine*, vol 19, no. 1, Jan. 2004, pp. 19-35.

[46] W. L. Melvin, "Space-time adaptive radar performance in heterogeneous clutter," *IEEE Transaction on Aerospace and Electronic Systems,* vol 36, no.2, pp 621-633, April 2000.

[47] W. Xu and M. Kaveh, "Analysis of the performance and sensitivity of Eigendecomposition-based detectors," *IEEE Trans. on signal processing,* vol. 43, no.6, Jun. 1995.

[48] X. Wang, H. Qi, H. Du, "Distributed source number estimation for multiple target detection in sensor networks," *IEEE Workshop on Statistical Signal Processing,* pp 395-398, MO, Sept. 2003.

[49] Y. D. Huang and M. Barkat, "On estimation of number of moving targets via frequency-diversity signaling," *Proceedings of the 32nd Midwest Symposium on Circuits and Systems,* vol.2, pp 1170-1173, Aug. 1989.

BIOGRAPHICAL STATEMENT

Hung Dinh Ly was born in Hatay, Vietnam in 1979. He received his B.S. degree from Posts and Telecommunications Institute of Technology, Vietnam in May 2002 and his M.S. degree from The University of Texas at Arlington in August 2007, both in Electrical Engineering. From June 2002 to July 2005, he was an Assistant Lecturer at the Department of Telecommunication Engineering, Posts and Telecommunications Institute of Technology. His current research interests include Information Theory, Signal Processing, Wireless Communications, and Sensor Networks. He is a student member of IEEE.